UDC 544.47, 546.791

DOI: 10.15372/CSD2021307

Depleted Uranium Compounds and Prospects for Their Use in Catalysis

Z. R. ISMAGILOV[1,2], N. V. SHIKINA[1]

[1]*Boreskov Institute of Catalysis, Siberian Branch of the Russian Academy of Sciences, Novosibirsk, Russia*

E-mail: zinfer1@mail.ru

[2]*Federal Research Center of Coal and Coal Chemistry, Siberian Branch of the Russian Academy of Sciences, Kemerovo, Russia*

(Received 22.02.21)

Abstract

The main directions of the utilization of depleted uranium compounds, modern trends in the use of uranium oxides and complex compounds based on them in catalytic processes, and methods for producing uranium oxides are considered in the review. It is shown that oxygenated uranium compounds are promising in all areas of catalysis, including environmental protection processes, organic synthesis, photocatalysis, electrocatalysis, processes for the production of hydrogen and valuable chemical compounds. The achievements of the Boreskov Institute of Catalysis SB RAS in the development of methods for the production of uranium oxides with different U/O ratios and uranium-containing catalysts for environmental protection and hydrogen production within the framework of the international program "Development of technology for the production of new effective catalysts based on raw materials from depleted uranium oxides" are described in detail. The review includes foreign and domestic publications from 1955 to 2021.

Keywords: depleted uranium compounds, uranium oxides, physicochemical properties of uranium oxides, uranium-containing catalysts

INTRODUCTION

Natural uranium consists mainly of uranium-238 (~99.3 %) and uranium-235 (~0.7 %) isotopes [1]. Today an overwhelming majority of reactors of nuclear power plants in the world use uranium fuel enriched in uranium-235 to a few percent. As a result of uranium enrichment a rich in uranium-235 uranium product is formed (used for the production of nuclear fuel) and depleted uranium in the form of hexafluoride (DUHF). Russia today has the most advanced uranium processing technologies that reduce the content of U-235 in the DUHF to 0.1 % and less (while foreign technologies attain a value of 0.2–0.3 %) [2]. The main issue nowadays discussed is can DUHF be considered a raw material or mainly radioactive waste? Basically, DUHF is considered a useful resource. In non-nuclear industries, fluorine-containing compounds are used in the production of ozone-safe freons and for etching printed circuit boards and chips. Depleted uranium is a promising material for doping semiconductors and magnetic materials, which can be used as catalysts in the oil industry, it can be used in areas where materials with high density are required, as ballast, as well as an "accumulator" of hydrogen for its storage. The depleted uranium is also used as an alloying when creating high-strength steels, the manufacture of containers for the transport of radioactive materials, and for construction materials of the shell of reactors on

fast neutrons. In this regard, the processing of DUHF represents scientific and commercial interest [2–6].

The results of the analysis of patent and scientific literature [7–31] give evidence on the intensification of work in the disposal of uranium hexafluoride (UF_6) and other compounds to obtain substances effective for practical applications. The patent subject-matters are mainly methods of obtaining stable uranium oxides from UF_6, waste or natural sources containing depleted uranium.

Among possible applications of uranium oxides or uranium complex compounds is their use in catalytic processes, which can be very diverse. The uniqueness of uranium oxide systems is due to the presence of a number of polymorphic modifications, several oxidation degrees and the existence of many compounds of variable composition and metastable phases [32, 33]. This served as an incentive to study uranium oxides as potential catalysts for various processes and initiated active patenting in the 80s and in the 90s of the previous century [34–51]. Uranium belongs to the actinide family the study of which in the last decade revealed a significant role of 5*f*-orbitals in the reactivity, superior to the lanthanide group and *d*-transition metals [52–55]. Chemical transformations with uranium participation, such as the six-electron reduction of N_2 to two reactive ammonia molecules or four-electron oxidation of water to oxygen under mild conditions, determine the prospects to create highly efficient heterogeneous catalysts based on depleted uranium. Due to the relatively large ion radius and the kinetic lability of coordination and oxidative states uranium contributes to the activation of small molecules, such as CO, CO_2, N_2, O_2, H_2O, CH_4, HCl and NH_3 [53]. One of the most important industrial processes using uranium compounds as a catalyst is the Haber–Bosch process. Haber [56] notes that uranium and uranium nitrides serve as effective catalysts for obtaining ammonia from N_2. Many publications are devoted to the study of the bimetal uranium complexes capable of binding nitrogen [57–62]. The participation of 5*f*-uranium orbitals in the formation of intermetallic bonds between transition metals and uranium was studied. Uranium's ability to activate small molecules predetermined the use of uranium complexes in the reactions of hydroamination, hydroxylation and polymerization of alkenes and alkynes [55, 63–66], ammoxidation of alkanes and alkenes [67–72], oxidation of hydrogen chloride to chlorine (Deacon process) [73–76]. Catalytic reactions with transformations of oxidized compounds on uranium catalysts may be impaired due to the strength of the U–O bond. However, the Eisen group conducted studies that showed the effectiveness of the compounds of U (IV) in the dimerization reactions of aldehydes (Tishchenko reaction) [77] and processes that became key approaches in the use of uranium catalysts for hydroalkoxylation reactions [78], the addition of alcohols to heterocumulene [79], polymerization with the opening of the epoxide [80] and ether [81] cycles and the dehydration of amides [82].

One of the interesting directions of the use of uranium-containing catalysts is the photocatalytic oxidation of organic impurities in the visible region of light. In [83, 84], porous supports (TiO_2, Al_2O_3, SiO_2) modified by uranyl nitrate showed high activity in the oxidation reaction of acetone. Using the XPS method, the authors revealed that the reduction of U^{6+} to U^{5+} is slow on the surface of Al_2O_3 and SiO_2, but on TiO_2 the transformation of U^{6+} to U^{4+} is rapid; and this is the reason of the higher activity of U–TiO_2 catalysts. The doping of anatase with uranium [85] determines the synergistic effect of the oxidative state of uranium and the width of the band gap of the support in the photocatalytic reaction of the oxidation of rhodamine B under visible light. The less the width of the band gap and the less is the amount of U^{6+}, the more active is the catalyst. Photocatalytic properties of uranium organometallic complexes in rhodamine degradation reactions [86, 87], organic dyes [88, 89], and antibiotic tetracycline [90, 91] are described. The authors of [92] synthesized a binuclear uranium complex with salen for CO_2 reduction to methanol. The assembly of two U-centres into one coordination group made it possible to form U-centres with distorted pentagonal bipyramid geometry. This design of the compounds provided a high rate of formation of MeOH (1.29 mmol/(g · h)) with a product yield of 18 %.

Uranium catalysts are successfully used to obtain light hydrocarbons and synthesis gas, as well as in organic synthesis. Thus, in [93], the possibility of using bimetallic Ca–U and Ca–Th catalysts for oxidative dimerization of methane with N_2O as an oxidizing agent was shown. The main reaction products were C_2-hydrocarbons (C_2H_4 and C_2H_6). In the case of bimetallic systems Ni–U–O, Ni–Th–O and Cu–Th–O [94], the behaviour of uranium and thorium catalysts in methane oxidation was different. The selectivity of uranium catalysts to C_2-hydrocarbons was higher than that of tho-

rium systems, which, in turn, turned out to be more effective in relation to CO and H_2 formation (selectivity of approximately 90 %). Uranium oxides U_3O_8 synthesized from four different complexes [95] were investigated in the reactions of oxidation of benzyl alcohol to benzaldehyde. The activity of catalysts depended on the morphology of uranium oxides and was higher on more dispersed samples. In the reduction of 4-nitrophenol to 4-aminophenol which is widely used as an intermediate product in pharmaceutics, agrochemistry, as dyes and pigments, the hybrid catalyst U–Pd/graphene [96] was shown to be very efficient. The introduction of uranium made it possible to significantly increase the activity of the Pd/graphene system due to the charge transfer between Pd and U and the higher Pd dispersion since uranium prevented palladium aggregation. The complex compounds of uranium are used for the synthesis of aniline [97], in the Diels–Alder reaction to obtain a substituted derivative of cyclohexene [98]. Catalysts in the form of uranyl complexes are known for the halogen-exchange reaction of alkyl halides with elementary iodine and bromine, providing a high yield of corresponding alkyl bromides and iodides [99], as well as for alkane fluorination reactions [100].

Such an important area of applying depleted uranium compound as electrocatalysis should be also mentioned. The reduction of oxygen and hydrogen peroxide are technologically important reactions in the field of energy production. Graphene hybrids with uranium and thorium compounds showed excellent electrocatalytic properties with respect to the reduction of oxygen and hydrogen peroxide [101, 102], which can indicate the enormous potential of these materials for use in the conversion of energy and in sensor devices. In uranium systems, a pair of UO_3–U_3O_8 oxides [101] as an active component, as well as individual oxide U_3O_8 [102] on graphene oxide demonstrated high activity in the reaction of hydrogen peroxide reduction and significantly greater stability than the commercial catalyst Pt/C. The results of another work [103] are rather debatable. In this work the electrochemistry of the redox pair $[U^{VI}O_2(CO_3)_3]^{4-}/[U^{V}O_2(CO_3)_3]^{5-}$ is examined in detail on the electrochemically reduced graphene oxide (ERGNO) glass carbon electrode (GC) in a saturated solution of Na_2CO_3 (pH ≈ 12.3). It was found that ERGNO can catalyze the redox reaction $[U^{VI}O_2(CO_3)_3]^{4-}/[U^{V}O_2(CO_3)_3]^{5-}$. However, no increase in the current in the ERGNO electrode compared with the unmodified GC electrode was observed for the same reaction, so this study was intended to substantiate the need to systematically study the electrochemistry of actinide elements on graphene materials to accelerate their use in the nuclear technology.

There are data on the study of uranium oxides or complex compounds of uranium in other areas. Uranium oxide UO_2 nanoparticles were synthesized by a special method via the preparation of uranyl organic gel in ethylene glycol followed by microwave-assisted decomposition. These nanoparticles exhibit semiconductor properties, have high sensitivity to various gases (NO_2, NH_3, CO) and ethanol [104], and can be used for gas sensors. Metallocene systems of uranium at room temperature are active in dehydrogenation of dimethylaminoboranes used as hydrogen storage systems. The authors made a bold conclusion that the activity of uranium complexes exceeds all dehydrogenation catalysts known in the literature [105].

Uranium compounds are used in catalytic processes and as catalyst supports. Thus, in [106, 107], the possibility of using U_3O_8 with a specific surface of 10–15 m^2/g as a support for Ni- and Ru-catalysts for the process of steam conversion of methane and a new ICAR process, for direct transformation of nuclear to chemical energy is shown. The method is based on a combination of both nuclear and catalytic reactors in one technological space by loading the catalyst directly into the active (energy-generating) zone of the nuclear reactor. The idea of this approach is based on the use of the energy dissipation of the ionizing particle into heat directly inside the catalyst granules, which ensures a very effective proceeding of the necessary energy-accumulating "thermochemical" reaction. Catalysts based on uranium oxide combining nuclear fuel and catalyst functions for chemical energy accumulation used in the ICAR method can provide significant intensification of the energy-accumulating chemical reaction and increase the specific energy load of the energy conversion to 100–150 kW/dm^3. In [108], uranium oxides UO_3 and U_3O_8, synthesized from uranyl nitrate, performed the role of a support for Au-catalysts of the process of steam conversion of CO to produce hydrogen. Conversion of CO on the Au/UO_3 catalyst was higher than on Au/U_3O_8 due to the UO_3 reducibility and a high concentration of gold atoms on the surface. The structure and catalytic properties of nanosized gold particles deposited on U_3O_8 by homogeneous deposition method were investigated in [109]. In the epoxidation of styrene by anhydrous *tert*-bu-

tylhydroperoxide, this catalyst was less active as compared to catalysts containing gold and oxides of other transition metals. Nevertheless, further studies of these systems have shown that the Au/U_3O_8 catalyst is quite effective in oxidizing benzyl alcohol [110].

It is difficult to list all the areas of catalysis that use depleted uranium compounds. There is a huge array of patent and scientific literature on the use of uranium in the reactions of organic synthesis, synthesis gas production, in the Fischer–Tropsch process, partial oxidation, hydrocracking, hydrotreating, oxidation of CO, hydrocarbons and selective reduction of nitrogen oxides. These chemical processes were analyzed and systematized in our previous reviews [111, 112].

The literature describes various ways to obtain uranium oxides, including a sol-gel method [104, 113, 114], precipitation methods, thermal decomposition, hydrothermal synthesis, electrolytic deposition. Preparation of uranium oxides by the sol-gel method in [104] was carried out stage by stage. At first, a uranyl nitrate solution was prepared by dissolution of uranium oxide powder in nitric acid. The uranium-containing gel was formed in ethylene glycol without the use of any organic gelation agent and easily turned into uranium dioxide nanoparticles of a uniform size (~4 nm) with the help of microwave treatment. In [113], uranyl nitrate was first obtained by dissolving uranium oxide powder in concentrated nitric acid. The obtained gel particles were washed with carbon tetrachloride, then with a 5 % NH_4OH solution, and dried in the air for 8 hours at 100 °C. Sols in the form of uranyl nitrate ascorbate [114] were obtained by adding ascorbic acid to a solution of uranyl nitrate hexahydrate, and alkalinisation with aqueous ammonium hydroxide, and then emulsification in 2-ethylhexane-1 containing 1 vol. % SPAN-80. Emulsion drops were gelled by water extraction with a solvent. The final stage was the calcination of the gel microspheres in the air to uranium octoxide (U_3O_8). The authors of [106] describe the method of synthesis of porous oxides of uranium U_3O_8 and UO_2 with a specific surface area of 10–15 m^2/g. Catalysts were obtained by the precipitation of ammonium polyuranate, followed by calcining in the air at 800 and 1000 °C to obtain U_3O_8 and in hydrogen medium at 600, 800 °C to obtain UO_2. The hydrothermal method using organic amines as reducing agents is described in [115]. The authors note the dependence of the morphology of UO_2 and U_3O_8 samples in the form of rods on the type of reagent, reducing agent and the concentration of solutions.

A new type of uranium-containing porous microspheres with a hierarchical nano/microstructure was successfully synthesized by a hydrothermal method without the use of template agents from uranyl nitrate hexahydrate, urea and glycerol [116]. The study of the formation mechanism of microspheres has shown that an intermediate compound $3UO_3 \cdot NH_3 \cdot 5H_2O$ is first formed, and then the hydrothermal product, which is transformed into uranium oxides (UO_{2+x}, U_3O_8 and UO_3). The hydrothermal synthesis without the use of a template was carried out by the authors of [117]. Spherical UO_2 nanoparticles with an average diameter from 30 to 250 nm and nanocubes U_3O_8 with a width of 400 nm and a length of 1 μm were obtained. For selective preparation of pure phase U_3O_8 and UO_2 nanoparticles, the experimental conditions were optimized, such as the pH and the temperature of the solution, as well as the concentration of the reducing agent – hydrazine. U_3O_8 nanoparticles were prepared by the template synthesis using Pluronic-123, *n*-butanol and 2-propanol as a surfactant and the co-surfactant, which were formed by nucleation, growth and subsequent aggregation of the solid phase in the solution [118]. Nanoparticles were covered *in situ* by an aqueous solution of tetraethylorthosilane. Studies have shown that U_3O_8 particles in the size range from 4 to 10 nm are distributed solely inside the silica matrix. The thermal decomposition method is used to obtain uranium oxides with specified properties. For this, complex compounds of uranium with various ligands affecting the morphology and the size of oxide particles were synthesized [95, 119]. Such methods for the preparation of uranium oxides are also known as the radiolytic reduction of uranyl ammonium tricarbonate [120], the method of electrospinning to obtain nanofibers of uranium oxides U_3O_8 and UO_2 with an unusually thin diameter from uranyl acetylacetonate in organic solvents and polymer carrier polyvinylpyrrolidone [121].

A series of works on the use of depleted uranium oxides for the preparation of catalysts for environmental protection and hydrogen production was carried out in the Laboratory of Environmental Catalysis of the Boreskov Institute of Catalysis SB RAS (BIC SB RAS). Studies were carried out to obtain bulk uranium oxides by various methods, individual oxides of uranium and their mixtures with transition metals supported on alumina were synthesized. The physicochemical and catalytic properties of the materials obtained depending on the synthesis conditions were studied.

The purpose of this review is a generalization of the obtained extensive data array.

BULK URANIUM OXIDES. PREPARATION AND PROPERTIES

Currently, most technological schemes for the synthesis of uranium oxides are based on the precipitation of ammonium polyuranates and their subsequent calcination to obtain U_3O_8. Samples of ammonium diuranate (ADU) are obtained by adding an aqueous solution of ammonia to a solution of uranyl nitrate to attain pH 11, and then a dense yellow precipitate is filtered, washed and dried to a constant mass. For ADU precipitation by ammonium hydroxide from the solutions of uranyl nitrate, the approximate formula of the product is usually considered as $(NH_4)_2U_2O_7$, but actually, the product has a nonstoichiometric composition. X-ray phase analysis shows that this sample corresponds to formula $(NH_4)_2 \cdot O \cdot 4UO_3 \cdot 7H_2O$ [122]. The thermal balance shows that this compound decomposes in several stages. A number of thermal effects are observed on the thermogram of ammonium diuranate: two endothermic (at 206 and 656 °C) and several exothermic. The effect at 206 °C corresponds to the removal of water, the exothermic one to the decomposition of diuranate (removal of ammonia and water, as well as the crystallization of the formed uranium trioxide). Further heating leads to the final transition of UO_3 in U_3O_8 (638 °C).

To obtain uranium oxides, uranyl nitrate hexahydrate ($UO_2(NO_3)_2 \cdot 6H_2O$) is the main precursor of uranium oxide catalysts. The decomposition of this compound into uranium trioxide proceeds in several stages. It is believed that the process occurs mainly via the following reactions:

$$UO_2(NO_3)_2 \cdot 6H_2O \leftrightarrow UO_2(NO_3)_2 \cdot 3H_2O + 3H_2O$$
$$UO_2(NO_3)_2 \cdot 3H_2O \leftrightarrow UO_2(NO_3)_2 \cdot 2H_2O + H_2O$$
$$UO_2(NO_3)_2 \cdot 2H_2O \leftrightarrow UO_2(NO_3)_2 + 2H_2O$$
$$2UO_2(NO_3)_2 \leftrightarrow 2UO_3 + 2N_2O_4 + O_2$$

For each stage, the constants of the equilibrium pressures and the heat of the transition are determined [123]. Uranyl nitrate forms three well-known hydrates containing six, three and two water molecules. Traditionally uranyl nitrate hexahydrate is used for the preparation of catalysts.

We synthesized the powders of bulk uranium oxides using various methods. The methods of preparation of bulk uranium oxides UO_2, U_4O_9 and U_3O_8 were developed by the salt electrolysis [124], which allows one to purposefully synthesize samples of uranium oxides with predetermined oxygen coefficients (O/U). To obtain uranium oxides with the required oxygen content, optimal electrolysis conditions were selected (the composition of the electrolyte, temperature and precipitation potential). To obtain UO_2, electrolysis was performed at a temperature of 900 °C (electrolyte, mol. %: 48.33 K_2WO_4 – 36.24 K_2WO_7 – 15.43 UO_2WO_4) in the potentiostatic mode with the precipitation potential −1.0 V in the air. U_4O_9 was obtained at a temperature of 800 °C (electrolyte: eutectic mixture $(Li,Na,K)_2SO_4$ – 30 mol. % UO_2SO_4; composition of the eutectic mixture, mol. %: 78.0 Li_2SO_4 – 8.5 Na_2SO_4 – 13.5 K_2SO_4) in the potentiostatic mode, the precipitation potential −1.0 V in the air, and U_3O_8 at a temperature of 900 °C (electrolyte, mol. %: 48.33 Na_2MoO_4 – 36.24 $Na_2Mo_2O_7$ – 15.43 UO_2MoO_4) in the potentiostatic mode with the precipitation potential −0.8 V in the air. The samples were characterized by XPS, TPR, TPO and EPR methods. It has been established that in the UO_2 and U_4O_9 precipitates the oxygen content exceeds the stoichiometric value due to surface forms of uranium oxides with a higher O/U ratio. Uranium oxides obtained by the method are plate crystals of the rectangular shape (Fig. 1).

Samples of uranium oxides were tested in the reaction of deep oxidation of C_4H_{10} (1 vol. % C_4H_{10} in the air, 1000 h^{-1}). The UO_2 sample is inactive in the reaction. Oxides U_4O_9 and U_3O_8 showed the same activity. The temperature of 50 % butane conversion over these samples was 480 °C.

In another work, uranium oxides were obtained by the precipitation method from an aqueous solution of UO_2 $(NO_3)_2 \cdot 6H_2O$ with 25 % of ammonia and by the thermal decomposition of the above salt [125]. Depending on the preparation conditions at different calcination temperatures, samples were obtained with various phase compositions (Table 1).

XRD studies have shown that after drying of the salt precipitated with ammonia, a highly dispersed complex compound $NH_3U_2O_6 \cdot 3H_2O$ was obtained. This compound decomposes at 300 °C to highly dispersed products, unidentified by the X-ray database of JCPDS. With further heating, the crystallization of products occurs, and after heat treatment at 500 °C, the phase β-UO_3 appears. The heat treatment at 600 °C and above leads to the formation of α-U_3O_8. The materials obtained are monophasic. The phase composition of the samples obtained by thermal decomposition varies from γ-UO_3 formed at 300 °C up to α-U_3O_8, produced at 600 °C and higher calcina-

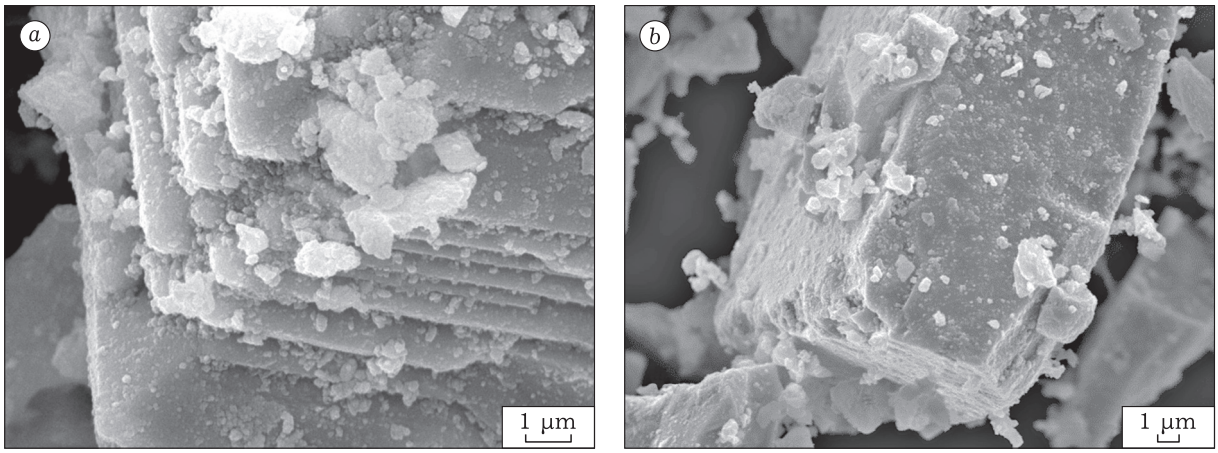

Fig. 1. SEM micrographs of uranium oxides U_3O_8 (*a*) and U_4O_9 (*b*) prepared by electrolysis of molten salts.

tion temperatures. In contrast to the deposition method, the thermal decomposition of uranyl nitrate leads to the formation of samples with nonuniform phase composition consisting of a mixture of various polymorphic modifications of uranium oxides.

Spectroscopic studies [125] complement the XRD data and provide the identification of phases of uranium oxides on the basis of the IR spectra. In the spectrum of uranyl nitrate (Fig. 2, *a*) bands at 740, 908 and 1384 cm^{-1} corresponding to the vibrations of the chains −U−O− [126], the stretching vibrations of the U=O bond in uranyl groups [127] and vibrations of nitrate groups [128] were observed. After the thermal decomposition of the salt at 300 and 500 °C, the sample spectra are characterized by a set of absorption bands at 469, 553, 872, 932 and 1384 cm^{-1}. The first two weak bands can be assigned to the vibrations of the U_3O_8 phase present in the sample in trace amounts. Bands at 872 and 932 cm^{-1} correspond to the vibrations of the UO_3 phase and the band at 1384 cm^{-1} to those of nitrates. The spectrum of the sample at 600 °C consists of bands characteristic of U_3O_8 phase (446, 489, 532 and 726 cm^{-1}). However, there are high-frequency bands 773 and 862 cm^{-1} in the spectrum, which may be related to the vibrations of the UO_3 phase. After thermal decomposition at 1000 °C, the only bands present in the spectrum are those characteristic of the phase U_3O_8. The data of IR spectroscopy confirm the XRD results on the heterogeneity of the phase composition of the samples obtained by the thermal decomposition of uranyl nitrate. IR spectra of the precipitated samples (see Fig. 2, *b*) contain bands assigned to one specific phase of uranium oxides: at 500 °C bands at 915, 969 and 820 cm^{-1} of the phase UO_3; at 600−1000 °C, a band at 740 cm^{-1}, which corresponds to the vibrations of the −U−O− chain, and a set of three bands in the region 540, 500, 460 cm^{-1} corresponding to U_3O_8.

The reduction of uranium oxides with hydrogen proceeds in two stages to form the same in-

TABLE 1

Dependence of the properties of uranium oxide on the methods of preparation and thermal treatment

T_{calc}, °C	Precipitation		Thermal decomposition	
	S_{BET}, m^2/g	Phase composition	S_{BET}, m^2/g	Phase composition
300	8.7	High-dispersed (<60 Å) unidentified phase, probably a mixture of products of thermal decomposition of $NH_3U_2O_6 \cdot 3H_2O$	3	γ-UO_3 or γ′-UO_3 probably, traces of α-$UO_{2.92}$
500	12.5	β-UO_3	7	γ-UO_3 or γ′-UO_3 probably, traces of β-UO_3
600	11	α-U_3O_8	1.7	α-U_3O_8 γ-UO_3 or γ′ − UO_3
800	3.4	α-U_3O_8	1.1	α-U_3O_8
1000	1.2	α-U_3O_8	0.18	α-U_3O_8 probably, traces of γ-U_3O_8

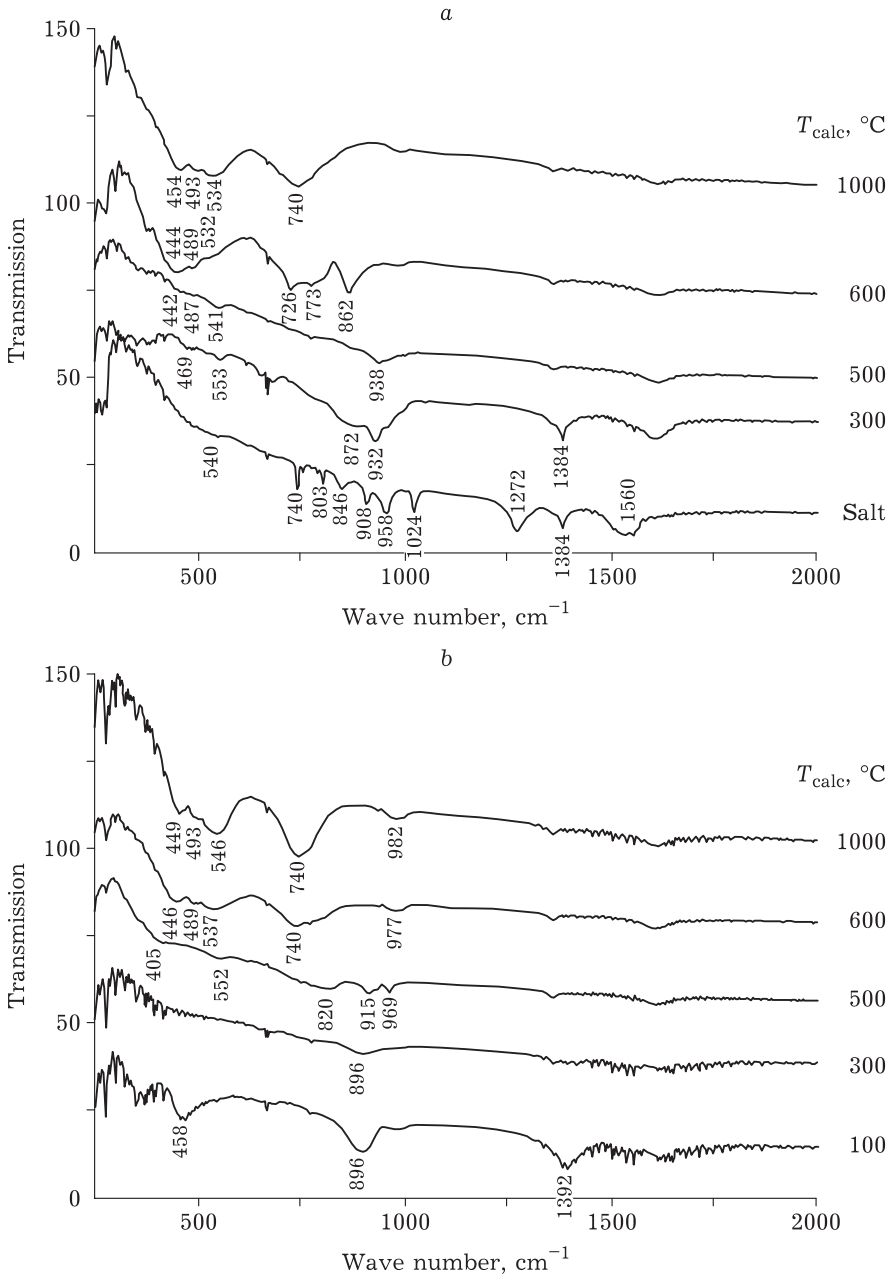

Fig. 2. IR spectra of bulk uranium oxides prepared by thermal decomposition (*a*) and precipitation (*b*) of uranyl nitrate (salt) at different temperatures.

termediate compound. Based on the study of samples by the TPR H_2 and calculations of the amount of absorbed hydrogen, the conclusion was made that uranium trioxide UO_3 and octaoxide U_3O_8 are reduced to uranium dioxide through an intermediate compound U_4O_9. The increase in the calcination temperature of the oxide U_3O_8 does not lead to a change in the phase composition, as shown by the XPS method, however, the TPR curves are shifted to the region of higher temperatures, which is associated with an increase in the size of uranium oxide particles as a result of sintering.

Samples prepared by various methods differ in particle sizes and morphology (Fig. 3) [129]. The sample obtained by the precipitation and calcined at a temperature of 500–600 °C (see Fig. 3, *a*) consists of fine crystallites in the form of plates with a thickness of 0.1–0.2 μm and a length up to 1 μm. With an increase in the calcination temperature during the sintering process, the particle size increases, and at 1000 °C, larger crystals

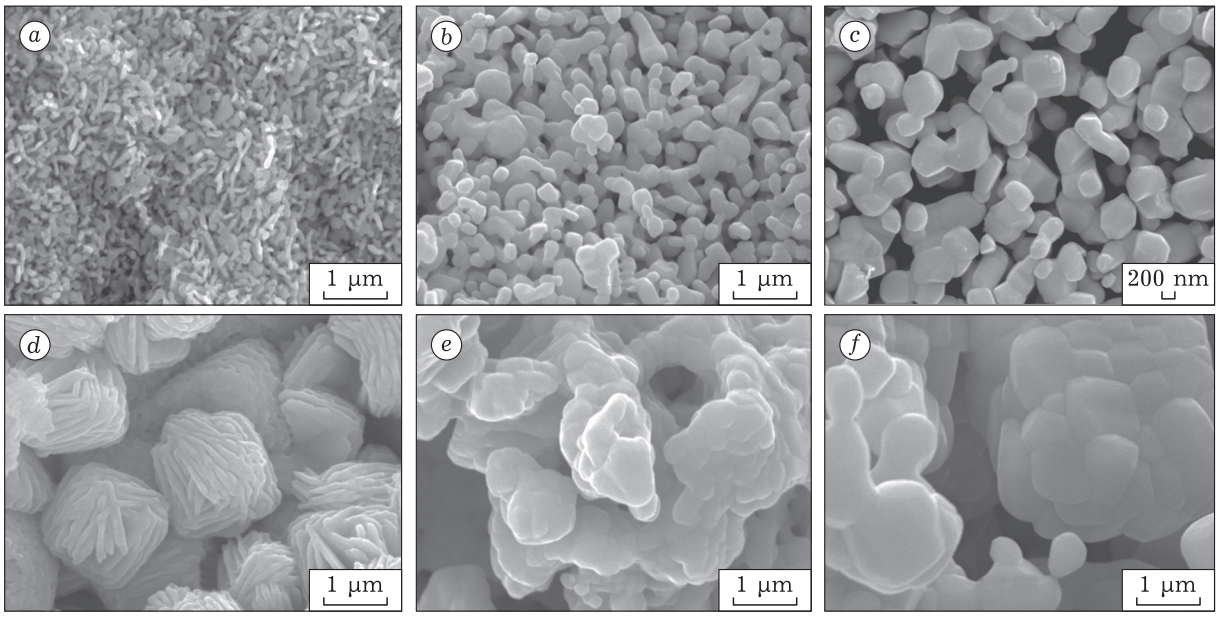

Fig. 3. Micrographs of the samples of bulk uranium oxides prepared by precipitation and calcined at 600 (*a*), 800 (*b*) and 1000 °C (*c*), or by the thermal decomposition of uranyl nitrate and calcined at 600 (*d*), 800 (*e*) and 1000 °C (*f*).

are formed with a size of 1 to 5 μm (see Fig. 3, *c*). The porous structure also changes, the pore size between the particles increases from 100 nm at 500 °C to tens of micrometres at 1000 °C. In thermal decomposition, larger crystals of oxides are formed compared to the precipitation method. On a micrograph of a sample of uranium oxide obtained by thermal decomposition of salt, already at 600 °C, large aggregates of up to 2 μm are observed, consisting of a set of plates oriented in various directions (see Fig. 3, *d*). With an increase in calcination temperature to 800 °C, the melting of the plates in the aggregates is observed, with the ingrowth of the aggregates and the formation of secondary pores 1 μm in size. Further increase in temperature to 1000 °C leads to sintering and the growth of uranium oxide crystals up to 5–7 μm (see Fig. 3, *f*). Pore sintering is accompanied by a decrease in the textural parameters of uranium oxides in both series, but the specific surface area of the samples obtained by the deposition method is higher compared to the method of thermal decomposition.

The studies of the properties of bulk uranium oxides make it possible to apply the results obtained to regulate the phase composition, the specific surface area and the morphology of samples by the synthesis conditions.

Uranium oxides obtained by the precipitation method and thermal decomposition were investigated in the reaction of deep oxidation of butane [125, 130]. Comparison of the temperatures of 50 % conversion of butane on two series of samples shows that uranium oxides obtained by the precipitation method are more active than uranium oxides obtained by the thermal decomposition of uranyl nitrate (Fig. 4). The degree of conversion of butane over the catalysts of both series decreases with an increase in the calcination temperature of the samples. These data, as well as the reaction of TPR with hydrogen, demonstrate the direct dependence of activity on the specific surface area of the oxides.

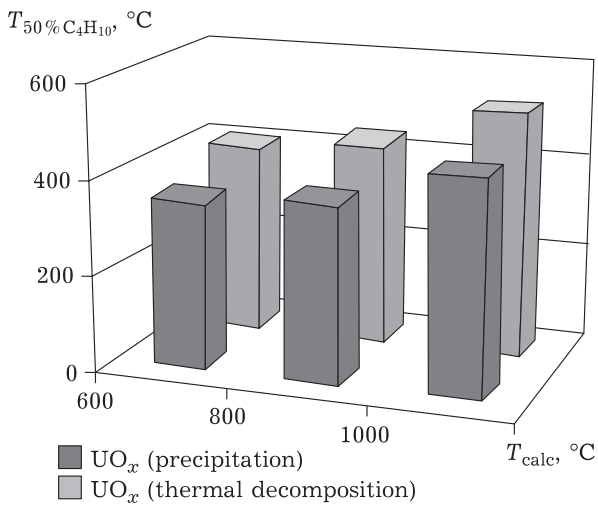

Fig. 4. Diagram of temperatures of 50 % butane conversion on UO_x-catalysts prepared by methods of precipitation and thermal decomposition and calcined at 600, 800, and 1000 °C.

SUPPORTED SINGLE-COMPONENT URANIUM OXIDE SYSTEMS. PREPARATION AND PROPERTIES

Uranium oxides deposited on various supports are characterized, as a rule, by more developed textural parameters compared to bulk oxides and are of great interest to catalysis. The uniqueness of such materials is the mutual influence of uranium oxides and support which is manifested in changing the properties of each component of the supported system. Thus, in the works of Ledoux with co-authors, it was shown that uranium compounds at proper impregnation can significantly improve the dispersion of aluminium oxide [131] and more than twice increase the SiC specific surface area [132]. Kumar and others used in their works a hydrothermal method of synthesis to prepare 1–6 mass % U on MCM-48 [113]. The introduction of the uranyl groups from solutions of acetic acid into the MCM-48 structure led to an increase in the lattice parameter, the degree of structuring and the pore size of the support.

Catalyst properties are often dependent on synthesis conditions. In [133, 134], we investigated 5 mass % U/Al_2O_3 catalysts prepared in three ways: 1) the incipient wetness impregnation of spherical γ-Al_2O_3; 2) the method of solid-phase synthesis of the powders of γ-Al_2O_3 (the same alumina as in method 1) and UO_3, obtained by the deposition method from aqueous solutions of uranyl nitrate [125, 130], followed by calcining solid-phase samples at 500–1000 °C for 4 h; 3) the method of mixing powders of support and uranium oxides preliminarily calcined at the same temperatures.

The work shows that the properties of the catalysts depend on the preparation method and are due to varying degrees of the interaction of the active component and the support. In the impregnated catalyst, the mutual influence of uranium and aluminium oxide compounds is significant and expressed in the absence of phases of uranium oxides as shown by the diffraction patterns of samples calcined up to 1000 °C (Table 2),

TABLE 2

Physicochemical properties of catalysts 5 % U-Al_2O_3 prepared by impregnation, solid phase synthesis and mechanical mixing

Catalyst	T_{calc}, °C	S_{BET}, m^2/g	Phase composition	Colour
Impregnated	500	160	γ-Al_2O_3 with lattice parameter a = 7.920 Å	Yellow-orange
	600	167	γ-Al_2O_3 with lattice parameter a = 7.920 Å	Yellow-orange
	900	78	δ-Al_2O_3 and γ-Al_2O_3	Yellow-brown
	1000	40	θ-Al_2O_3; most probably, α-U_3O_8, however the presence of α-$UO_{3.01}$ or α-$UO_{2.92}$ is possible	Gray-beige
	1000, 18 h	32	θ-Al_2O_3, trace amounts of α-Al_2O_3, α-U_3O_8 with particle size exceeding 400 Å	Gray-green
	1100	33	θ-Al_2O_3; trace amounts of a-Al_2O_3; α-U_3O_8 with particle size exceeding 400 Å, the presence of α-$UO_{3.01}$ or α-$UO_{2.92}$ is possible	Gray-green
Solid-phase	500	156	γ-Al_2O_3; β-UO_3 with particle size exceeding 400 Å	Yellow
	600	140	γ-Al_2O_3; trace amounts of β-UO_3 with particle >400 Å; α-U_3O_8 with particle >400 Å	Green
	900	95	δ+γ-Al_2O_3; α-U_3O_8 with particle >400 Å	Gray
	1000	70	δ+γ-Al_2O_3; α-U_3O_8 with particle >400 Å	Light gray
Mixed	500	156	γ-Al_2O_3; β-UO_3 with particle >400 Å	Yellow
	600	163	γ-Al_2O_3; α-U_3O_8 with particle >500 Å	Green
	900	104	δ+γ-Al_2O_3; α-U_3O_8 with particle >500 Å	Dark gray
	1000	75	δ+γ-Al_2O_3; α-U_3O_8 with particle >500 Å	Light gray

TABLE 3

Dependence of the phase composition of 5 % U/Al_2O_3 catalysts on the nature of uranium oxide precursor at different calcination temperatures

T_{calc}, °C	Phase Composition		
	Precursors		
	Uranyl nitrate	Uranyl oxalate	Uranyl acetate
100	γ-Al_2O_3	γ-Al_2O_3; $(C_2O_2)_3U \cdot 3H_2O$	γ-Al_2O_3
300	γ-Al_2O_3	γ-Al_2O_3; high-dispersed phase expressed as a halo in the 2θ region 29–33°	γ-Al_2O_3
500	γ-Al_2O_3	γ-Al_2O_3; α-$UO_{3.01}$	γ-Al_2O_3
600	γ-Al_2O_3	γ-Al_2O_3; α-U_3O_8	γ-Al_2O_3
800	γ-Al_2O_3	γ-Al_2O_3; δ-Al_2O_3 (traces); α-U_3O_8	δ-Al_2O_3 (traces); g-Al_2O_3
900	δ-Al_2O_3; γ-Al_2O_3	γ-Al_2O_3; δ-Al_2O_3; α-U_3O_8	δ-Al_2O_3; γ-Al_2O_3
1000	θ-Al_2O_3; α-U_3O_8, α-$UO_{3.01}$ or α-$UO_{2.92}$	θ-Al_2O_3; α-Al_2O_3 (traces); α-U_3O_8	θ-Al_2O_3; α-Al_2O_3 (traces); α-U_3O_8

while in a series of catalysts prepared by methods 2 and 3, uranium oxides are registered at all calcination temperatures of samples from 500 to 1000 °C. In the impregnated series of samples calcined at 1000 °C, the interaction phase is destroyed with the formation of highly dispersed uranium oxides. With increasing the temperature and duration of calcination, the size of particles of uranium oxides and the degree of crystallinity increases.

The content of the U_3O_8 phase calculated from the calibration plots of mechanical mixtures by the XRD method in samples of different catalysts calcined at 1000 °C is different and is equal to 20, 30 and 100 % of the introduced amount in impregnated, solid-phase and mixed samples, respectively. This is explained by the fact that in the solid-phase catalyst, the mutual influence of uranium and aluminium oxides is expressed significantly less than in the impregnated one, and in a mixed sample, the interaction of uranium oxides and aluminium oxides is practically absent. The phase state of the support in samples of the solid-phase and mixed catalyst (1000 °C) is characterized by a mixture of low-temperature forms (γ + δ)-Al_2O_3, while in the impregnated catalyst, the high-temperature form θ-Al_2O_3 is found. This means that the interaction of uranium oxide with the support contributes to polymorphic transformations of the low-temperature forms of aluminium oxide to the high-temperature θ-modification.

The phase of the interaction of uranium and aluminium oxides is probably the type of solid solutions with a limitation by the amount of a dissolved phase. So, with an increase in the concentration of uranium oxides to 15 % in the impregnated catalysts, uranium oxides that are not included in the alumina crystal lattice are formed as a separate phase at 800 °C.

The genesis of the phase composition of the catalyst during thermal treatment depends on the precursors – uranium salts. Uranyl nitrate $UO_2(NO_3)_2$, uranyl acetate $UO_2(OOCCH_3)_2$ and uranyl oxalate $UO_2C_2O_4$ were used as precursors [135]. It has been established that catalysts obtained from nitrate and acetate salts are characterized by similar phase composition at the same calculation temperatures (Table 3). On the diffraction patterns of these catalysts, reflexes belonging to the phases of uranium oxides are found only after calcining the samples at 1000 °C. Unlike them, in catalysts obtained from oxalate, the UO_3 phase appears already at 500 °C.

The influence of uranium oxides on the state of the alumina support was elucidated in the study of impregnated samples by the HRTEM method [133]. It was shown that on the surface of 5 % U/Al_2O_3, calcined at 600 °C, the uranium ions are formed in the super dispersed state on the surface of the crystallites γ-Al_2O_3 (Fig. 5, *a*), after increasing the calcination temperature to 1000 °C, there is an ordering of the uranium ions on the support surface (see Fig. 5, *b*). The presence of uranium particles on the surface of the support crystallites is confirmed by the EDX analysis (the spectra are not given). The study of the HRTEM also revealed an unusual behaviour of supports γ- and θ-Al_2O_3 containing uranium surface ions. The radiation-thermal effect of a high-intensity electron beam changes the morphology of the support particles, causing diffuse mass transfer of the material. In aluminium oxide particles, hol-

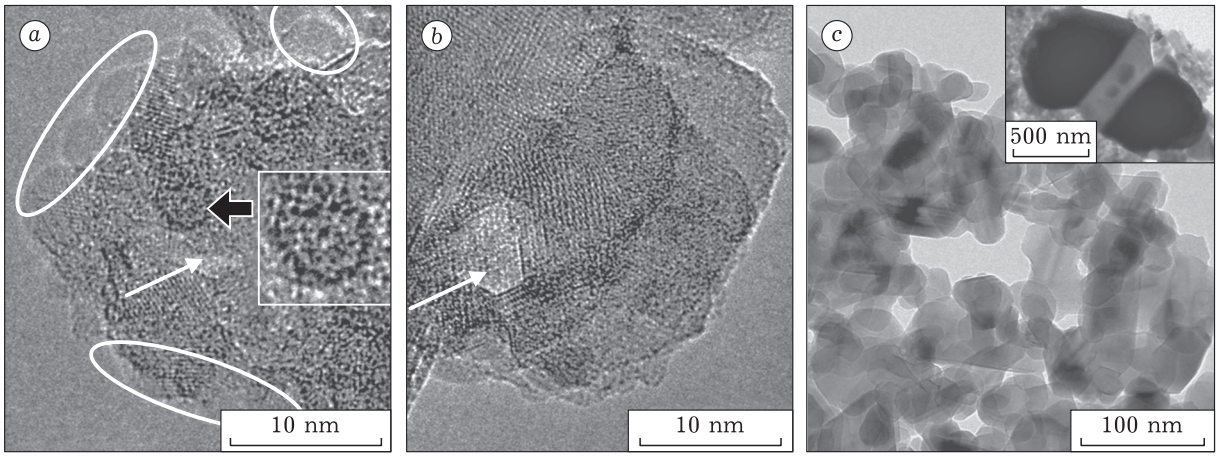

Fig. 5. TEM images of 5 % U/Al_2O_3 catalyst calcined at 600 (*a*), 1000 (*b*) и 1100 °C (*c*).

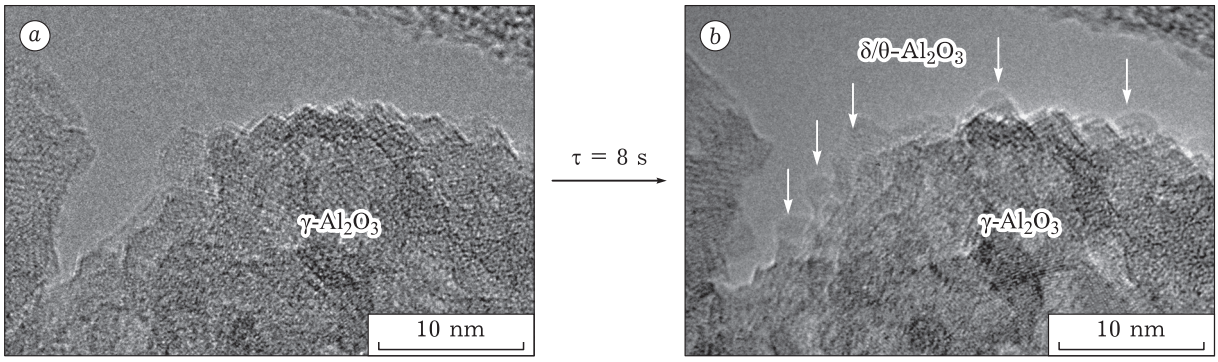

Fig. 6. TEM images of 5 % U/Al_2O_3 catalyst calcined at 600 °C. Redistribution of the support material under the action of electron beam: *a* – at the beginning of video recording, *b* – at 8 s since the beginning of video recording.

low areas are formed (shown by white arrows in Fig. 5, *a*, *b*). At the same time, spherical formations of aluminium oxide of up to 5 nm appear in the near-surface layers of the support (shown by white ovals in Fig. 5, *a*).

Figure 6 shows TEM images obtained by video recording the process of the redistribution of the support material under the influence of an electron beam on the sample 5 % U/Al_2O_3 (*a* – the image at the beginning of the shooting, *b* – after 8 s from the shooting), and the creation of spherical formations in the near-surface layers of the support is shown (marked with white arrows). The high energy of the electron beam also causes the phase conversion of alumina in these spherical formations, since the study shows the presence of δ-Al_2O_3 or θ-Al_2O_3 in them, unlike the remaining surface of the particle represented by γ-Al_2O_3 (see Fig. 6).

A similar phenomenon was also detected for a sample calcined at 1000 °C (see Fig. 5, *b*), except that the same high-temperature modification θ-Al_2O_3 was observed on the initial surface of the particles and on the resulting bulges. Such changes were not detected in the study of pure Al_2O_3 without uranium, although the electron beam had the same intensity. In this paper, the observed phenomenon was not investigated in detail; however, it is obvious that the reinforced regrouping of the material of the support takes place, initiated by an electron beam, and it is due primarily to the presence of U ions in the crystal lattice of alumina. It is possible that U ions penetrate into the lattice filling vacant cationic positions in γ-Al_2O_3 or replacing alumina ions in θ-Al_2O_3, which destabilizes the crystal alumina lattice and increases the diffusion mass transfer. It should be noted that such changes in the support morphology can cause the effect of reducing the temperature of polymorphic phase transitions of alumina in impregnated catalysts. At the next temperature of the calcination – 1100 °C, according to the TEM, the support contains not only particles of θ-Al_2O_3, but also spherical particles of α-Al_2O_3 with a size of 50–100 nm (not shown in the Figure). Hollow areas are not formed also in θ-Al_2O_3 crystallites exposed to an

electron beam. Uranium oxide is present in this sample in the form of α-U_3O_8 particles with a size from 100 nm (see Fig. 5, *c*) to larger spliced aggregates of 2–3 μm in size (see Fig. 5, *c*, the insert). Thus, the calcination at 1100 °C leads to a sharp transition of U from an ion state in θ-Al_2O_3 to a state of macrocrystalline oxide phases with a predominance of the α-U_3O_8 phase (see Table 2).

The behaviour of U/Al_2O_3 catalysts in the TPR H_2 reaction attracts interest. Catalysts prepared by the methods of solid-phase synthesis and mixing are reduced by hydrogen in a predictable way. With an increase in calcination temperature, the reduction peaks shift to the high-temperature region. For impregnated catalysts, anomalous behaviour is observed. The higher the calcination temperatures of the samples, the easier they are reduced, *i.e.*, more reactive forms of the state of the active component appear. The XPS study indicates a sharp increase in the surface concentration of uranium taking place when the calcination temperature is increased to 1000 °C, which is mainly due to the dispersion of uranium oxide.

The effect of thermoactivation of the 5 % U/Al_2O_3 catalyst synthesized by the impregnation method in the experiments of the TPR H_2 manifests itself in its high activity in the reactions of deep oxidation of hydrocarbons. The activity of uranium oxides on Al_2O_3 in the oxidation reactions of butane and methane is determined by a number of factors, including the specific surface area, the state of the active component and support, the dispersion of uranium oxides. In a series of impregnated samples, an increase in the activity with an increase in the calcination temperature is observed. Among the studied samples, the catalyst calcined at 1000 °C is the most active, due to the formation of a highly active state of uranium oxides on the surface of the support, established by the methods of XRD, TEM and XPS. Further increase in the temperature and in the duration of calcination, contributing to the consolidation of particles of the active component and reduction of the specific surface area of the catalysts, naturally lead to a decrease in their activity. The chemical nature of the precursors also affects the activity of UO_x deposited on alumina. The testing of the catalysts prepared from nitrate, acetate and oxalate of uranyl showed that the catalyst originated from nitrate was most active in the reaction of deep oxidation of butane and the least active was the oxalate sample [135]. The basis of this dependence is the features of phase formation of supported catalysts (see Table 3) and the dispersion of the formed α-U_3O_8 phase.

SUPPORTED TWO-COMPONENT UO_x-MeO_x/AL_2O_3 (Me: Ni, Co, Mo, Cr) CATALYTIC SYSTEMS. PREPARATION AND PROPERTIES

The works of British scientists G. J. Hutchings and S. Taylor in the middle and late 1990s became breakthrough and showed the prospects of uranium oxides in the reaction of low-temperature catalytic oxidation of volatile organic compounds (VOC), including chloroorganic compounds [136–148]. Catalysts are characterized not only by high activity but also thermal stability and resistance to the poisoning effects of halogens, sulphur compounds and water vapour. The introduction of modifying additives of transition metal oxides (Co, Cu, Cr, *etc.*) increased the activity of uranium oxide catalysts, while selectivity to CO_2 increased almost to 100 %.

We have conducted a series of works on the development of two-component catalysts containing transition metal oxide as one component and uranium oxide as a second one for various catalytic processes. In [149, 150], the modification of uranium oxide supported on alumina by nickel was performed by sequential impregnation of alumina with an aqueous solution of uranyl nitrate ($UO_2(NO_3)_2 \cdot 6H_2O$) and after calcination at 500 and 1000 °C by a nickel nitrate solution. The catalysts were calcined at 850 °C in air. The content of uranium in catalysts varied from 0 to 30 mass %, and the nickel content was equal to 10 mass %. The phase composition of the Ni-U/Al_2O_3 catalysts did not differ from the samples of individual uranium oxides deposited on alumina (see Table 2, impregnated catalysts). In samples containing a small amount of uranium oxides (<5 mass %), the α-U_3O_8 phase was not observed. This phase was detected only with an increase in the content of uranium in the sample over 15 mass %. Despite the sufficiently large content of Ni in catalysts (10 mass %), the NiO oxide phases and metal Ni were not detected, since the high calcination temperature of the catalyst (850 °C) contributed to the transfer of Ni into the composition of solid solutions based on the structure of γ-Al_2O_3. The specific surface area of catalysts depended on the number of components introduced into the support and on preparation conditions. With an increase in the calcination temperature of intermediate U/Al_2O_3 samples and an increase in the concentration of uranium oxides, the specific surface area predictably decreased.

TABLE 4

Characteristics of the activity of catalysts (yields of H_2, CO and carbon) in the reaction of methane reforming with carbon dioxide

Catalyst	Yield, %	Temperature of the reaction, °C	
		800	850
Ni/Al_2O_3	H_2	18	22
	CO	18	17
	Carbon	14	14
Ni-5 % $U(1000)/Al_2O_3$	H_2	11	17
	CO	12	16
	Carbon	5	7
Ni-15 % $U(1000)/Al_2O_3$	H_2	5	17
	CO	10	23
	Carbon	0	1.5
Ni-30 % $U(1000)/Al_2O_3$	H_2	8	22
	CO	13	26
	Carbon	0	0.4

The $Ni\text{-}U/Al_2O_3$ catalysts were investigated in steam and carbon dioxide reforming reactions of methane and in the reaction of methane partial oxidation. In the study of the activity of the samples, the dependence of the catalytic parameters (the conversion of methane, the yield of the reaction products) on the specific surface area was not found. In the reaction of methane steam reforming, the presence of uranium in the Ni-catalyst contributed to an increase in the catalytic activity, the higher the activity, the more uranium contained the catalyst. On a sample containing 30 mass % U, the activity increased with increasing reaction temperature, reaching the maximum value at 850 °C (the CH_4 conversion was equal to 77 %). Catalysts calcined at 1000 °C after the stage of uranium deposition before the nickel introduction had higher activity compared to catalysts obtained from samples U/Al_2O_3, calcined at 500 °C (the CH_4 conversion is 47 % at 850 °C). The effect of thermal activation of catalysts in the reaction of steam reforming of methane, as in the reactions of deep oxidation of hydrocarbons, is associated with high dispersion of uranium oxides in the samples of U/Al_2O_3 calcined at 1000 °C.

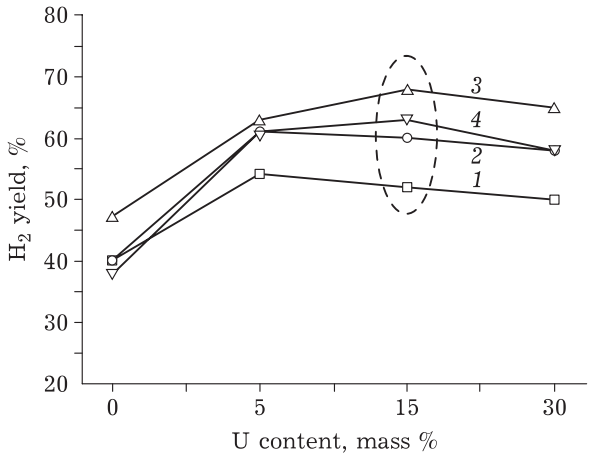

Fig. 7. The dependence of the hydrogen yield in the reaction of partial oxidation of methane on the uranium content in the catalyst $10Ni\text{-}U/Al_2O_3$ at temperatures, °C: 700 (*1*), 750 (*2*), 800 (*3*) and 850 (*4*).

The main problem in the development of catalysts for the process of methane reforming with carbon dioxide is the deactivation of catalysts as a result of coke formation. The study of $Ni\text{-}U/Al_2O_3$ catalysts in the reaction of carbon dioxide reforming of methane under conditions: C_{CH_4} = 20 vol. %, C_{CO_2} = 20 vol. %, space velocity 45 000 h^{-1}, showed that the addition of uranium into the Ni-containing catalyst significantly reduces the amount of coke formed in the reaction, with about the same hydrogen yield (Table 4). The carbon yield observed at 850 °C decreases from 14 % for the catalyst that does not contain uranium to 0 % for the catalyst containing 30 mass % uranium. Thus, the modification of the Ni/Al_2O_3 catalyst with uranium suppresses the side process of the coke formation and thereby significantly increases the service life of the catalyst.

In the reaction of partial oxidation of methane (POM), the promoting effect of uranium oxide additives is also established. The introduction of uranium into the traditional catalysts of POM based on nickel makes it possible to increase the yield of hydrogen (Fig. 7), which over the urani-

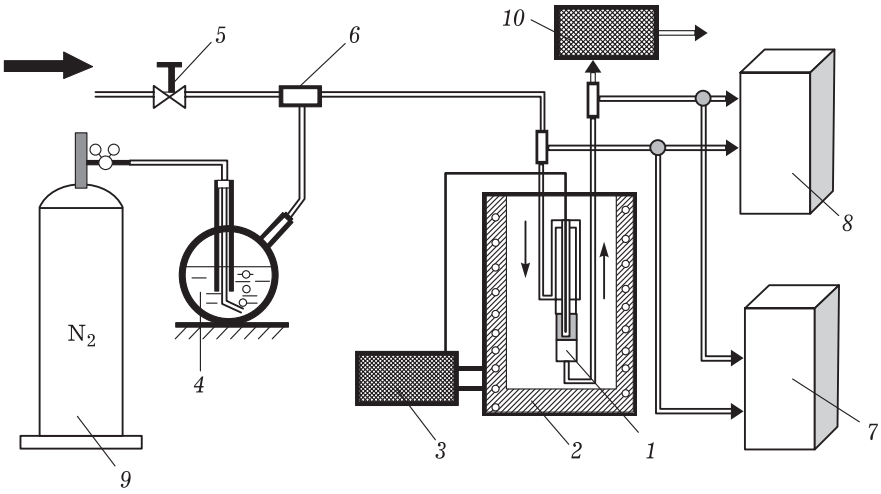

Fig. 8. The scheme of a laboratory setup for studying catalytic oxidation of chlorine-containing compounds: *1* – catalytic reactor; *2* – electric heater; *3* – temperature regulator; *4* – saturator; *5* – regulating valve; *6* – mixer; 7, *8* – gas chromatographs; *9* – N_2 cylinder; *10* – aerosol filter.

um-containing catalysts reaches 68 % compared with 40 % for an analogue of the industrial catalyst Ni/Al_2O_3, under the same testing conditions (800 °C, a space velocity of 50 000 h^{-1}, the composition of the reaction mixture 20 vol. % CH_4 + 10 vol. % O_2 + Ar). The activity of Ni-U/Al_2O_3 catalysts in the POM increases with increasing temperatures from 550 to 800 °C, regardless of the uranium content (0–30 masss %). Above 800 °C, a slight decrease in the catalyst activity is observed. The long-term tests of Ni-U/Al_2O_3 catalysts at 800 °C showed their stability due to the resistance of catalysts to coking [135].

Industrial emissions of hydrocarbons and chlorine-containing organic compounds have always been the focus of attention. As known, chlorine-containing pollutants are stable and can be destroyed at temperatures above 1000 °C, this process leads to the formation of highly toxic by-products – dioxins and dibenzofurans. Catalytic combustion at low temperatures more effectively oxidizes pollutants without the formation of by-products. It is known that commercial catalysts based on noble metals are quickly deactivated in such processes [151]. Hutchings and co-workers in their publications [139–141] showed that uranium oxide catalysts are not deactivated in the oxidation of hydrocarbons, and their chlorine-containing derivatives.

The process of oxidation of chlorobenzene (see the reaction equation) on the uranium-containing catalysts was investigated by us in [152–155].

$C_6H_5Cl + 7O_2 = 6CO_2 + HCl + 2H_2O$

Initially, we studied the oxidation of chlorobenzene and trichloroethylene by air on the one-component catalysts 5 % U/Al_2O_3 and 15 % U/Al_2O_3 [152]. The reaction was carried out at a temperature of 200–550 °C, space velocities 10 000–70 000 h^{-1} and a concentration of chlorobenzene up to 11 g/m^3 in the laboratory setup (Fig. 8). It was shown that 5 % U/Al_2O_3 and 15 % U/Al_2O_3 catalysts could effectively oxidise chlorinated volatile organic compounds at a temperature of 450–500 °C. The selectivity with respect to CO_2 was 98–100 %. The formation of molecular chlorine, phosgene and other toxic chlorine-containing compounds in the reaction products was not observed.

Then, the process of oxidation of chlorobenzene on two-component catalytic systems was investigated [152–155]. Catalysts 7 mol. % U–7 mol. % Me (where Me is Cu, Cr, Mn, Co) on the granules γ-Al_2O_3 were prepared by the method of sequential impregnation of the support with solutions of uranyl nitrate hexahydrate, and after drying at 100 °C with solutions of nitrate salts $Cu(NO_3)_2 \cdot 3H_2O$, or $Cr(NO_3)_3 \cdot 9H_2O$, or $Mn(NO_3)_2 \cdot 6H_2O$, or $Co(NO_3)_2 \cdot 6H_2O$. A series of catalysts not containing uranium were synthesized for comparison: 7 mol. % Cu/γ-Al_2O_3, 7 mol. % Cr/γ-AL_2O_3, 7 mol. % Mn/γ-Al_2O_3, and 7 mol. % Co/γ-Al_2O_3, by impregnating alumina granules with the solutions of nitrate salts of the corresponding metals. All catalysts were calcined at 600 °C.

The addition of uranium oxide to transition metal oxide catalyst led to a significant increase in

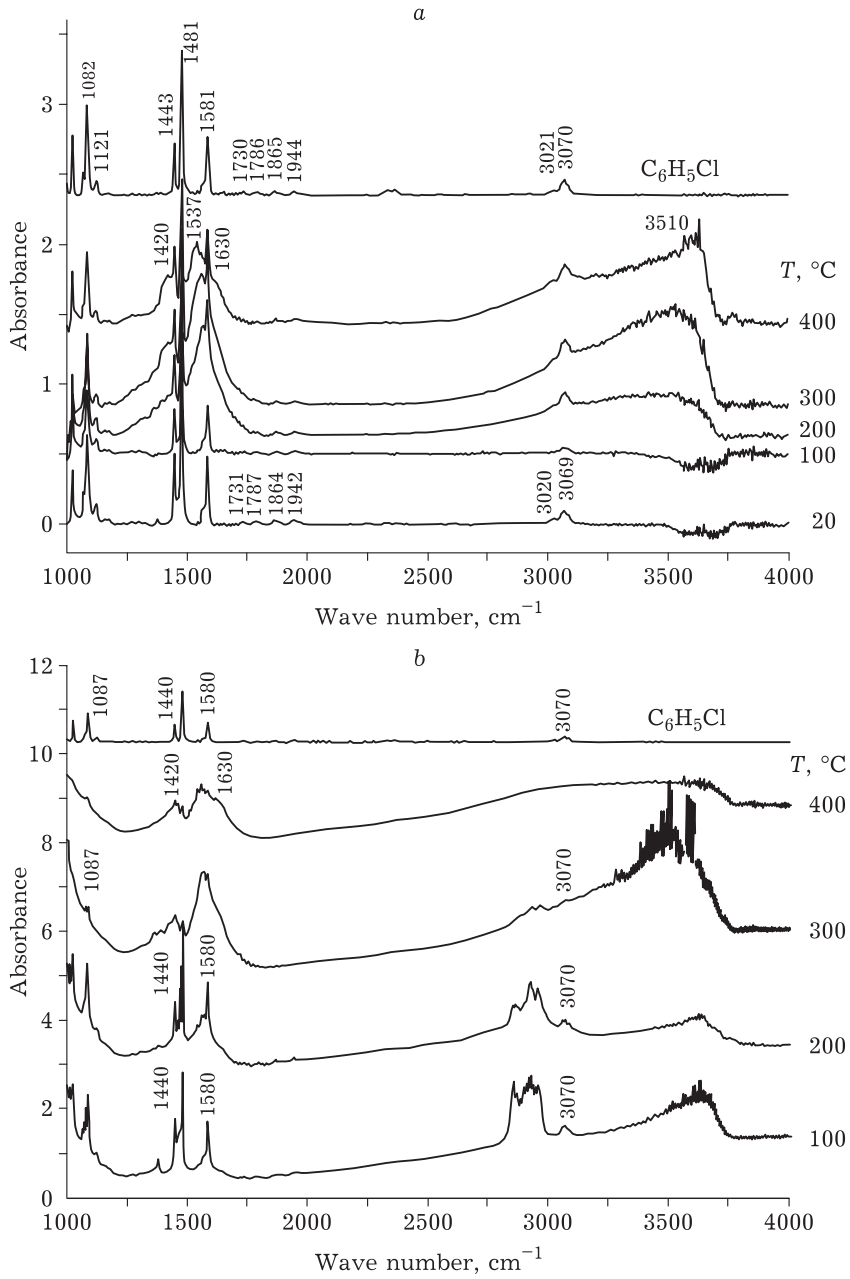

Fig. 9. IR spectra of chlorobenzene adsorbed on catalysts 7 mol. % U–7 mol. % Mn/γ-Al_2O_3 (*a*) and 7 mol. % Mn/γ-Al_2O_3 (*b*).

activity in the oxidation of chlorobenzene compared with one-component catalysts based on only transition metal oxides. The promoting effect of the introduction of uranium oxides to transition metal oxides was due to the formation of the phase of interaction in the form of uranates of the corresponding metals, which turned out to be much more active than simple oxides. Two-component Cr-U and Mn-U catalysts containing $Cr_2U_2O_9$/$UCrO_4$ and α-MnU_3O_{10}/β-MnU_3O_{10} uranate phases were even more active than the commercial catalyst based on the $MgCr_2O_4/Al_2O_3$ spinel (IC-12-72) with a difference of $T_{50\,\%}$ per 100 °C. The selectivity of uranium catalysts on CO_2 was 100 % at 450–500 °C.

The data on the IR spectroscopy of chlorobenzene adsorption (Fig. 9) on the catalysts shows that the oxidation of chlorobenzene on the uranium-containing catalysts (see Fig. 9, *a*) begins at a temperature of 200 °C (band at 1638 cm^{-1}, which is attributed to the vibrations of molecular water, and wide bands at 1400 and 1520 cm^{-1}, corresponding to vibrations of surface carbonate groups formed during chlorobenzene oxidation), which is

by 100 °C lower than on catalysts that do not contain uranium components (see Fig. 9, *b*).

The studied two-component uranium-containing catalysts can be arranged in the following sequence according to their activity: Cu-U/Al_2O_3 <Co-U/Al_2O_3 <Mn-U/Al_2O_3 <Cr-U/Al_2O_3. A very slight decrease in the conversion of chlorobenzene (by 4–5 %) was observed during the operation of catalysts at 500 °C for 40 hours. After long-term tests, the absorption of chlorine by the catalysts was less than 0.2 % of the total chlorine coming into the reactor [152].

Thus, it can be concluded that two-component catalysts 7 mol. % U–7 mol. % Me that showed high activity and stability in the oxidation reaction of chlorobenzene can be promising systems for cleaning gas emissions from chlorinated volatile organic compounds.

CONCLUSION

This review discusses publications concerning the studies of uranium oxygen compounds as catalysts. The analysis of the literature showed that uranium-containing catalysts are promising in all areas of catalysis, including environmental protection processes, organic synthesis, photocatalysis, electrocatalysis, processes for the production of hydrogen and valuable chemical compounds. Uranium catalysts are characterized by high stability and resistance to the adverse effects of catalytic poisons, which allows them to be used in processes accompanied by the release of chlorine, sulphur, water vapour, *etc*. The uniqueness of the uranium oxide systems is due to the presence in the U–O system of polymorphic modifications, several oxidation degrees and the existence of a variety of compounds of variable composition, stable and metastable phases. Due to the relatively large ion radius, the kinetic lability of coordination and oxidative states, uranium contributes to the activation of small molecules (for example, CO, CO_2, N_2, O_2, H_2O, CH_4, HCl and NH_3), which leads to the use of uranium-containing catalysts in many industrial processes, such as the Haber–Bosch process for the production of ammonia from nitrogen, Deacon process for chlorine production, ammoxidation of propylene, etc. The trend of research in recent years has become the use of uranium metal complexes, in which organic ligands provide high dispersion of active centres and excellent performance in various catalytic reactions.

The review describes in detail the work on the use of depleted uranium oxides for the preparation of catalysts conducted in BIC SB RAS in the Laboratory of Environmental Catalysis in collaboration with the Siberian Chemical Combine (Seversk), NGPII "VNIPIET" (Novosibirsk), and the Institute of High-Temperature Electrochemistry UB RAS (Ekaterinburg). The researchers systematically investigated methods of preparing bulk and supported uranium oxides, the prospects for the use of uranium compounds as catalysts in the processes of deep oxidation of hydrocarbons, partial oxidation of methane, steam and carbon dioxide reforming of methane, and oxidation of chlorinated volatile organic compounds.

It should be noted that all the work carried out in BIC SB RAS was organized in accordance with the requirements of the "Basic sanitation regulations for radiation security" (OSPORB-99/2010), taking into account all issues of toxicity [156], radiation safety [157, 158] and the rules of accounting and control of nuclear materials [159]. At the same time, the maximum permissible concentrations (MPC) of U-238 are determined only by its chemical toxicity and are 0.075 mg/m^3 in the air of the working area and 15 mg/L in the form of soluble compounds [156]. According to MPC standards, compounds of metals such as Ni, Cu, Zn are more toxic than U, and the MPC of these metals is 1.5 times lower. A common prejudice on the danger of depleted uranium compounds is greatly exaggerated and in the case of the strict fulfilment of the OSPORB rules, the work with depleted uranium compounds is no different from working with other chemical reagents.

Acknowledgements

The work was accomplished with the financial support of the ISTC (project No. 2799 "Development of technology for the production of new efficient catalysts based on raw materials from depleted uranium oxides"), and RAS in the framework of the integration project between SB RAS and UB RAS No. 7.

The authors express sincere gratitude to the employee of Federal Research Center of Coal and Coal Chemistry SB RAS (Kemerovo) N. Nalimova for the search for patents and scientific literature and the employees of BIC SB RAS (Novosibirsk) S. V. Lazareva, V. V. Kuznetsov, A. A. Gavrilova, M. A. Kerzhentsev; NGPII "VNIPIET" (Novosibirsk) Yu. V. Ostrovsky, M. Zabortsev; the Institute of High-Temperature Electrochemistry UB RAS (Ekaterinburg) V. K. Afonishkin; Siberian Chemical Combine (Seversk) V. A. Matyukha, V. G. Balakhonov, V. V. Lazarchuk for active participation in the research.

REFERENCES

1 G. T. Seaborg, J. J. Katz (Eds.), The Actinide Elements, 1st ed., New York, 1954.
2 Nikitin A., Muratov O., Vakhrusheva K., in: Depleted uranium hexafluoride. Current situation, issues of safe handling and prospects, E. Verevkina (Ed.), Izd-vo EPTs "Bellona", ANO assistance to environmental protection «Expert-Legal Center "Ecopravo"», 2020. (in Russ).
3 Muratov O. E., Handling problems of depleted uranium hexafluoride (review), *Teor. Prikl. Ekol.*, 2020, No. 4, P. 13–21. (in Russ.).
4 Bleise A., Danesi P.R., Burkart W., Properties, use and health effects of depleteduranium (DU): A general overview, *J. Env. Rad.*, 2003, Vol. 64, No. 2–3, P. 93–112.
5 Bekman I. N., Uranium. Course for Students, Izd-vo MSU, Moscow, 2009. (in Russ).
6 Betti M., Civil use of depleted uranium, *J. Env. Rad.*, 2003, Vol. 64, No. 2–3, P. 113–119.
7 Pat. US No. 5723100, 1998.
8 Pat. US No. 5901338, 1999.
9 Pat. US No. 5918106, 1999.
10 Pat. US No. 4963294, 1989.
11 Pat. US No. 4830841, 1989.
12 Pat. US No. 4397824, 1983.
13 Pat. US No. 3765844, 1973.
14 Pat. Eur No. 0148707, 1985.
15 Pat. US No. 3978194, 1976.
16 Pat. RU No. 2603359, 2016.
17 Pat. RU No. 2599528, 2016.
18 Pat. RU No. 2626854, 2017.
19 Pat. RU No. 2625979, 2017.
20 Pat. RU No. 2614712, 2017.
21 Afonichkin V. K., Khrustova L. G., Komarov V. E., Consecutive recovery of uranium oxides from uranyl-containing molten alkali metal sulfate electrolytes, *Russ. J. Inorg. Chem.*, 2013, Vol. 58, No. 4, P. 456–462.
22 Afonichkin V. K., Khrustova L. G., Komarov V. E., Continuous recovery of uranium oxides by electrolysis of M_2MoO_4-$M_2Mo_2O_7$-UO_2MoO_4 melts (M = Li, Na, K, Cs), *Russ. J. Appl. Chem.*, 2013, Vol. 86, No. 2, P. 133–140.
23 Magomedbekov E. P., Chizhevskaya S. V., Zhukov A. V., Polenov G. D., Klimenko O. M., Solid-phase conversion of depleted uranium tetrafluoride to oxides using mechanoactivated quartz, *Advances in Chemistry and Chemical Technology*, 2019, Vol. 33, No. 1 (211), P. 49–50. (in Russ).
24 Magomedbekov E. P., Chizhevskaya S. V., Klimenko O. M., Davydov A. V., Zhukov A. V., Chekmarev A. M., Sarychev G. A., Depleted uranium hexafluoride – technogenic raw material for obtaining high-purity inorganic fluorides, *At. Energy*, 2012, Vol. 111, No. 4, P. 282–287.
25 Polenov G. D., Chizhevskaya S. V., Zhukov A. V., Magomedbekov E. P, Solid-phase conversion of depleted uranium tetrafluoride into oxides using mechanoactivated quartz with the addition of sodium fluoride, *At. Energy*, 2017, Vol. 122, No. 5, P. 346–352.
26 Collier N., Harrison M., Brogden M., Hanson B., Release of uranium from candidate wasteforms, *Miner. Mag.*, 2012, Vol. 76, No. 8, P. 2939–2948.
27 Baranska J. A., Sadowski Z., Bioleaching of uranium minerals and biosynthesis of UO_2 nanoparticles, *Physicochem. Probl. Miner. Process.*, 2013, Vol. 49, P. 71–79.
28 Asta M. P., Beller H. R., O'Day P. A., Anaerobic dissolution rates of U(IV)-oxide by abiotic and nitrate-dependent bacterial pathways, *Environ. Sci. Technol.*, 2020, Vol. 54, No. 13, P. 8010–8021.
29 Atia B. M., Gado M. A., Cheira M. F., Kinetics of uranium and iron dissolution by sulfuric acid from Abu Zeneima ferruginous siltstone, Southwestern Sinai, Egypt, *Euro-Mediterr J. Environ. Integr.*, 2018, Vol. 3, Art. 39.
30 Kenzhaliev B. K., Surkova T. Y., Berkinbayeva A. N., Dosymbayeva Z. D., Chukmanova M.T., To the question of recovery of uranium from raw materials, *News of the National Academy of Sciences of the Republic of Kazakhstan. Series of Geology and Technical Sciences*, 2019, Vol. 1, No. 433, P. 112–119.
31 Kenzhaliyev B. K., Rkova T. Y. S., Berkinbayeva A. N., To the question of the intensification of the processes of uranium extraction from refractory raw materials, *Metalurgija*, 2019, Vol. 58, No. 1–2, P. 75–78.
32 Maiorov A. A., Braverman I. B., Technology for Producing Ceramic Uranium Dioxide Powders, Energoatomizdat, Moscow, 1985. (in Russ).
33 Katz J. J., Seaborg G. T., Morss L. R. (Eds), The Chemistry of the Actinides, 2nd ed., Chapman & Hall, London, 1986.
34 Pat. US No. 4581344, 1986.
35 Pat. US No. 4227993, 1980.
36 Pat. US No. 4487851, 1984.
37 Pat. US No. 4663305, 1987.
38 Pat. US No. 4755536, 1988.
39 Pat US. No. 5756419, 1998.
40 Pat. US No. 5130114, 1992.
41 Pat. US No. 3929624, 1975.
42 Pat. US No. 4402868, 1983.
43 Pat. US No. 4487850 , 1984.
44 Pat. US No. 5808143, 1998.
45 Pat. US No. 4375425, 1983.
46 Pat. US No. 4018712, 1977.
47 Pat. GB No. 1240633, 1971.
48 Pat. DE No. 19807079, 1999.
49 Pat. DE No. 19746210, 1999.
50 Pat. DE No. 19753817, 1999.
51 Pat. DE No. 19751046, 1999.
52 Kaltsoyannis N., Recent developments in computational actinide chemistry, *Chem. Soc. Rev.*, 2003, Vol. 32, No. 1, P. 9–16.
53 Leduc J., Frank M., Jürgensen L., Graf D., Raauf A., Mathur S., Chemistry of actinide centers in heterogeneous catalytic transformations of small molecules, *ACS Catal.*, 2019, Vol. 9, No. 6, P. 4719–4741.
54 Lu J. B., Ma X. L., Wang J. Q., Jiang Y. F., Li Y., Hu H. S., Xiao H., Li J., The *df–d* dative bonding in a uranium–cobalt heterobimetallic complex for efficient nitrogen fixation, *Inorg. Chem.*, 2019, Vol. 58, No. 11, P. 7433–7439.
55 Fox A., Bart S., Meyer K., Cummins C.C., Towards uranium catalysts, *Nature*, 2008, Vol. 455. P. 341–349.
56 Pat. DE No. 229126, 1909.
57 Cloke G. F. N., Hitchcock P. B., Reversible binding and reduction of dinitrogen by a uranium(III) pentalene complex, *J. Am. Chem. Soc.*, 2002, Vol. 124, No. 32, P. 9352–9353.
58 Odom A. L., Arnold P. L., Cummins C. C., Heterodinuclear uranium/molybdenum dinitrogen complexes, *J. Am. Chem. Soc.*, 1998, Vol.120, No. 23, P. 5836–5837.
59 Mansell S. M., Kaltsoyannis N., Arnold P. L., Small molecule activation by uranium tris(aryloxides): Experimental and computational studies of binding of N_2, coupling of CO, and deoxygenation insertion of CO_2 under ambient conditions, *J. Am. Chem. Soc.*, 2011, Vol. 133, No. 23, P. 9036–9051.
60 Evans W. J., Kozimor S. A., Ziller J. W., A monometallic *f*-element complex of dinitrogen: $(C_5Me_5)_3U(\eta^1\text{-}N_2)$, *J. Am. Chem. Soc.*, 2003, Vol. 125, No. 47, P. 14264–14265.
61 Roussel P., Scott P., Complex of dinitrogen with trivalent uranium, *J. Am. Chem. Soc.*, 1998, Vol. 120, No. 5, P. 1070–1071.
62 Falcone M., Chatelain L., Scopelliti R., Živković I., Mazzanti M., Nitrogen reduction and functionalization by a multi-

metallic uranium nitride complex, *Nature*, 2017, Vol. 547, P. 332–335.
63 Liu H., Ghatak T., Eisen M. S., Organoactinides in catalytic transformations: Scope, mechanisms and Quo Vadis, *Chem. Commun.*, 2017, Vol. 53, P. 11278–11297.
64 Monsigny L., Thuery P., Berthet J. C., Cantat T., Breaking C–O bonds with uranium: Uranyl complexes as selective catalysts in the hydrosilylation of aldehydes, *ACS Catal.*, 2019, Vol. 9, No. 10, P. 9025–9033.
65 Mansell S. M., Bonnet F., Visseaux M., Arnold P. L., Uranium(IV) amido-borohydrides as highly active diene polymerisation catalysts, *Dalton Trans.*, 2013, Vol. 42, No. 25, P. 9033–9039.
66 Fang J., Walshe A., Maron L., Baker R. J., Ring-opening polymerization of epoxides catalyzed by uranyl complexes: An experimental and theoretical study of the reaction mechanism, *Inorg. Chem.*, 2012, Vol. 51, No. 16, P. 9132–9140.
67 Pat. US No. 3983054, 1976.
68 Pat. US No. 4487850, 1984.
69 Pat. Eur No. 0121032, 1984.
70 Pat. US No. 5808143, 1998.
71 Pat. Eur No. 0072962, 2000.
72 Pat. US No. 6916763, 2004.
73 Pat. US No. 20100202959, 2010.
74 Pat. US No. 20110180419, 2011.
75 Amrute A. P., Krumeich F., Mondelli C., Perez-Ramirez J., Depleted uranium catalysts for chlorine production, *Chem. Sci.*, 2013, Vol. 4, No. 5, P. 2209–2217.
76 Krumeich F., Amrute A. P., Mondelli C., Perez-Ramirez J., Structural changes of a U_3O_8/ZrO_2 catalyst during HCl oxidation a HAADF-STEM study, *ZAAC*, 2014, Vol. 640, No. 5, P. 768–773.
77 Andrea T., Barnea E., Eisen M. S., Organoactinides promote the tishchenko reaction: The myth of inactive actinide-alkoxo complexes, *J. Am. Chem. Soc.*, 2008, Vol. 130, No. 8, P. 2454–2455.
78 Wobser S. D., Marks T. J., Organothorium-catalyzed hydroalkoxylation/cyclization of alkynyl alcohols. Scope, mechanism, and ancillary ligand effects, *Organometallics*, 2012, Vol. 32, No. 9, P. 2517–2528.
79 Batrice R. J., Kefalidis C. E., Maron L., Eisen M. S., Actinide-catalyzed intermolecular addition of alcohols to carbodiimides, *J. Am. Chem. Soc.*, 2016, Vol. 138., No. 7, P. 2114–2117.
80 Baker R. J., Walshe A., New reactivity of the uranyl ion: Ring opening polymerisation of epoxides, *Chem. Commun.*, 2012, Vol.48, No. 7, P. 985–987.
81 Walshe A., Fang J., Maron L., Baker R. J., New mechanism for the ring-opening polymerization of lactones? Uranyl aryloxide-induced intermolecular catalysis, *Inorg. Chem.*, 2013, Vol. 52, No. 15, P. 9077–9086.
82 Enthaler S., Straightforward uranium-catalyzed dehydration of primary amides to nitriles, *Chem. Eur. J.*, 2011, Vol. 17, No. 34, P. 9316–9319.
83 Filippov T. N., Kovalevskiy N. S., Solovyeva M. I., Chetyrin I. A., Prosvirin I. P., Lyulyukin M. N., Selishchev D. S., Kozlov D. V., *In situ* XPS data for the uranyl-modified oxides under visible light, *Data in Brief* , 2018, Vol. 19, P. 2053–2060.
84 Filippov T. N., Svintsitskiy D. A., Chetyrin I. A , Prosvirin I. P., Selishchev D. S., Kozlov D. V., Photocatalytic and photochemical processes on the surface of uranyl-modified oxides: An *in situ* XPS study, *Appl. Catal. A.General*, 2018, Vol. 558, P. 81–90.
85 Liu Y., Becker B., Burdine B., Sigmon G. E., Burns P. C., Photocatalytic decomposition of Rhodamine B on uranium-doped mesoporous titanium dioxide, *RSC Adv.*, 2017, No. 7, P. 21273–21280.
86 Liang L.-L., Hu Y-Q., Zhao J.-S., Two uranium coordination polymers constructed by a polycarboxylic acid: Structural variation, photoluminescent and photocatalysis properties, *J. Solid State Chem.*, 2020, Vol. 282, Art. 121085.
87 Tong X., Wang S., Zuo J., Ge Y., Gao Q., Liu S., Ding J., Liu F., Luo J., Xiong J., Two 2D uranyl coordination complexes showing effective photocatalytic degradation of Rhodamine B and mechanism study, *Chin. Chem. Lett.*, 2021, Vol. 32, No. 2, P. 604–608.
88 Jennifer S. J., Jana A. K., Influence of pyrazine/piperazine based guest molecules in the crystal structures of uranyl thiophene dicarboxylate coordination polymers: Structural diversities and photocatalytic activities for the degradation of organic dye, *Cryst. Growth. Des.*, 2017, Vol. 17, No. 10, P. 5318–5329.
89 Yue Z., Lin J., Silver M. A., Han L., Li X, Zhou J., Guo X., Bao H., Huang Y.-Y., Wang J.-Q., Anionic uranyl oxyfluorides as a bifunctional platform for highly selective ion-exchange and photocatalytic degradation of organic dyes, *Dalton Trans.*, 2018, Vol. 47, No. 42, P. 14908–14916.
90 Ren Y.-N., Xu W., Si Z.-X., Zhou L.-X., Zheng Y.-Q., Photocatalytic degradation of tetracycline antibiotics under visible light using uranyl isophthalate coordination polymers, *Polyhedron*, 2018, Vol. 152, P. 195–201.
91 Ren Y.-N., Xu W., Zhou L.-X., Zheng Y.-Q. Two new uranyl complexes as visible light driven photocatalysts for degradation of tetracycline, *Polyhedron*, 2018, Vol. 139, P. 63–72.
92 Azam M., Kumar U., Olowoyo J. O., Al-Resayes S. I., Trzesowska-Kruszynska A., Kruszynski R., Islam M. S., Khan M. R., Adil S. F., Siddiqui M. R., Al-Harthi F. A., Alinzi A. K., Wabaidur S. M., Siddiqui M. R., Shaik M. R., Jain S. L., Farkhondehfaldand M. A., Hernandez S., Dinuclear uranium(VI) salen coordination compound: An efficient visible-light-active catalyst for selective reduction of CO_2 to methanol, *Dalton Trans.*, 2020, Vol. 49, P. 17243–17251.
93 Branco J. B., Ferreira A. C., Leal J. P., Light hydrocarbons production over bimetallic calcium-actinide oxide catalysts using N_2O as oxidant , *J. Mol. Catal. A. Chem.*, 2014, Vol. 390, P. 45–51.
94 Branco J. B., Ferreira A. C., do Rego A. M. B., Ferraria A. M., Almeida-Gaschet T., Conversion of methane over bimetallic copper and nickel actinide oxides (Th, U) using nitrous oxide as oxidant, *ACS Catal.*, 2012, Vol. 2, No. 12, P. 2482–2489.
95 Majumder I., Chatterjee S., Fischer R. C., Neogi S. K., Mautner F. A., Chattopadhyay T., Syntheses of U_3O_8 nanoparticles form four different uranyl complexes: Their catalytic performance for various alcohol oxidations, *Inorganica Chim. Acta*, 2017, Vol. 462, P. 112–122.
96 Ding L., Zhang Z. Y., Li Y., Synthesis and catalytic property of urania-palladium-graphene nanohybrids, *Sci. China Mater.*, 2017, Vol. 60, No. 5, P. 399–406.
97 Ritter S., Uranium doubles up as a catalyst, *Chem. Eng. News*, 2017, Vol. 95, No. 49, P. 11.
98 Robinson J. R., Carroll P. J., Walsh P. J., Schelter E. J., Uranium(IV) BINOLate heterobimetallics: Synthesis and reactivity in an asymmetric Diels–Alder reaction, *Organometallics*, 2013, Vol. 32, No. 5, P.1493–1499.
99 Naeimi H., Nazifi Z. S., Uranyl Schiff base complexes as new heterogeneous catalysts for halogen exchange reactions between alkyl halides and elemental halogens, *Russ. Chem. Bull.*, 2015, Vol. 64, No. 8, P. 1814–1818.
100 Zhan X., Li P., Krzyaniak M., Knapp J., Wasielewski M. R., Farha O. K., Stabilization of photocatalytically active uranyl species in a uranyl-organic framework for heteroge-

neous alkane fluorination driven by visible light, *Inorg. Chem.*, 2020, Vol. 59, No. 23, P. 16795–16798.
101 Sofer Z., Jankovský O., Simek P., Klímová K., Machová A., Pumer, M., Uranium- and thorium-doped graphene for efficient oxygen and hydrogen peroxide reduction, *ACS Nano*, 2014, Vol. 8, P. 7106–7114.
102 Gao D. L., Zhang Z. Y., Ding L., Yang J., Li Y., Preparation and electrocatalytic properties of triuranium octoxide supported on reduced graphene oxide, *Nano Res.*, 2015, Vol. 8, No.7, P. 546–553.
103 Guin S. K., Ambolikar A. S., Kamat J. V., Reduced graphene oxide: Is it a promising catalyst for the electrochemistry of $[UO_2(CO_3)_3]^{4-}/[UO_2(CO_3)_3]^{5-}$?, *Electrochim. Acta*, 2015, Vol. 174, P. 1002–1008.
104 Ding L., Leduc J., Fischer T., Mathur S., Li Y., Gelation of uranyl ions and gel-derived uranium oxide nanoparticles for gas sensing, *Nanoscale Adv.*, 2020, Vol. 2, No. 6, P. 2478–2484.
105 Erickson K. A., Kiplinger J. L., Catalytic Dehydrogenation of dimethylamine borane by highly active thorium and uranium metallocene complexes, *ACS Catal.*, 2017, Vol. 7, No. 7, P. 4276–4280.
106 Gordeeva L. G., Aristov Yu. I., Moroz E. M., Rudina N. A., Zaikovskii V. I., Tanashev Yu. Yu., Parmon V. N., Preparation and study of porous uranium oxides as supports for new catalysts of stream reforming of methane, *J. Nucl. Mater.*, 1995, Vol. 218, No. 2, P. 202–209.
107 Aristov Yu. I., Tanashev Yu. Yu., Prokopiev S. I., Gordeeva L. G., Parmon V. N., ICAR process (immediate catalytic accumulation of ionizing radiation energy) as a new promising approach to the development of cheminuclear power plants, *Int. J. Hydrog. Energy.*, 1993, Vol. 18, No. 1, P. 45–62.
108 Dong Y. Y., Liao W. P., Suo Z. H., Uranium oxide-supported gold catalyst for water-gas shift reaction, *Fuel Process. Technol.*, 2015, Vol. 137, P. 164–169.
109 Patil N. S., Uphade B. S., McCulloh D. G., Bhargava S. K., Choudhary V. R., Styrene epoxidation over gold supported on different transition metal oxides prepared by homogeneous deposition-precipitation, *Catal. Commun.*, 2004, Vol. 5, No. 11, P. 681–685.
110 Choudhary V., Jha R, Jana P., Solvent-free selective oxidation of benzyl alcohol by molecular oxygen over uranium oxide supported nano-gold catalyst for the production of chlorine-free benzaldehyde, *Green Chem.*, 2007, Vol. 9, No. 3, P. 267–272.
111 Ismagilov Z. R., Kuntsevich S. V., Catalysts containing depleted uranium compounds, *Chemistry for Sustainable Development,* 2009, Vol. 17, No. 5, P. 439–463.
112 Ismagilov Z. R., Lazareva S. V., Synthesis and characterization of uranium-containing catalysts, *Catal. Rev.*, 2013, Vol. 55, No. 2, P. 135–209.
113 Kumar N., Bamankar Y. R., Pillai K. T., Mukerje S. K., Vaidya V. N., Venugopal V., Effect of feed solution composition and heat treatmentconditions on the morphology of uranium oxidemicrospheres prepared by sol-gel process, *J. Nucl. Mater.*, 2006, Vol. 359, No. 1–2, P. 80–92.
114 Brykala M., Deptula A., Rogowski M., Lada W., Olczak T., Wawszczak D., Smolinski T., Wojtowicz P., Modolo G., Synthesis of microspheres of triuranium octaoxide by simultaneous water and nitrate extraction from ascorbate-uranyl sols, *J. Radioanal. Nucl. Chem.*, 2014, Vol. 299, P. 651–655.
115 Wang Q., Li G.-D., Xu S., Li J.-X., Chen J.-S., Synthesis of uranium oxide nanoparticles and their catalytic performance for benzyl alcohol conversion to benzaldehyde, *J. Mater. Chem.*, 2008, Vol. 18, No. 10, P. 1146–1152.
116 Wang L., Zhao R., Wang C.-Z., Yuan L.-Y., Gu Z.-J., Xiao C.-L., Wang S.-A., Wang X.-W., Zhao Y.-L., Chai Z.-F., Shi W.-Q., Template-free synthesis and mechanistic study of porous three-dimensional hierarchical uranium-containing and uranium oxide microspheres, *Chem. Eur. J.*, 2014, Vol. 20, No. 39, P. 12655–12662.
117 Zhao R., Wang L., Gu Z.-J., Yuan L.-Y., Xiao C.-L., Zhao Y.-L., Chai Z.-F., Shi W.-Q., A facile additive-free method for tunable fabrication of UO_2 and U_3O_8 nanoparticles in aqueous solution, *CrystEngComm.*, 2014, Vol. 16, No. 13, P. 2645–2651.
118 Hasan S., Ghosh T. K., Synthesis of silica-coated uranium oxide nanoparticles by surfactant-templated sol-gel process for use as catalysts, *Nuclear Technology*, 2013, Vol. 181, No. 2, P. 371–379.
119 Beirakhov A. G., Rotov A. V., Efimov N. N., Il'in E. G., Gekhman A. E., Thermal Stability and products of decomposition of hydroxylaminate uranyl complexes, *Russ. J. Inorg. Chem.*, 2019, Vol. 64, P. 185–189.
120 Wang Y. M., Chen Q. D., Shen X. H., One-step synthesis of hollow UO_2 nanospheres via radiolytic reduction of ammonium uranyl tricarbonate, *Chin. Chem. Lett.*, 2017, Vol. 28, No. 2, P. 197–200.
121 Kundrat V., Patak A., Pinkas J., Preparation of ultrafine fibrous uranium dioxide by electrospinning, *J. Nucl. Mater.*, 2020, Vol. 528, Art. 151877.
122 Ball M. C., Birkett C. R. G., Brown D. S., Jaycock M. J., The thermal decomposition of ammonium diuranate, *J. Inorg. Nucl. Chem.*, 1974, Vol. 36, No. 7, P. 1527–1529.
123 Gromov B. V., Introduction to the Chemical Technology of Uranium. Textbook for Institutes of Higher Education, Atomizdat, Moscow, 1978. (in Russ.).
124 Afonichkin V. K., Khrustova L. G., Komarov V. E., Ismagilov Z. R., Kuznetsov V. V., Shikina N. V., Kuntsevich S. V., Rogov V. A., Synthesis of monophase uranium oxides UO_2, U_4O_9, U_3O_8 of specified composition by electrolysis of oxide salt melts and investigation of their physico-chemical and catalytic properties, International Conference "Catalysis: Fundamentals and Application" (Proceedings), Novosibirsk, Russia, July 4–8, 2007, P. 162–163.
125 Ismagilov Z. R., Lazareva S. V., Shikina N. V., Kuznetsov V. V., Kerzhentsev M. A., Ostrovsky Y. V., Rudina N. A., Rogov V. A., Ushakov V. A., Preparation and characterization of bulk uranium oxides for catalysis, *Mendeleev Commun.*, 2011, Vol. 21, P. 209–211.
126 Allen G. C., Crofts J. A., Infrared spectroscopy of the uranium/oxygen system , *J. Nucl. Mater.*, 1976, Vol. 62, No. 2–3, P. 273–281.
127 Kumar D., Bera S., Tripathi A. K., Dey G. K., Gupta N. M., Uranium oxide nanoparticles dispersed inside the mesopores of MCM-48: Synthesis and characterization, *Microporous Mesoporous Mater.*, 2003, Vol. 66, No. 2–3, P. 157–167.
128 Mishchenko K. P., Ravdel A. A. (Eds.), Brief Reference of Physical and Chemical Quantities, Issue 7, Chimiya, Leningrad, 1974. (in Russ.).
129 Shikina N. V., Kuntsevich S. V., Kuznetsov V. V., Ismagilov Z. R., New uranium oxide catalysts for VOC control, 10th International Symposium on Heterogeneous Catalysis (Proceedings), Varna, Bulgaria, Aug. 23–27, 2008, P. 28.
130 Kuntsevich S. V., Ismagilov Z. R., Shikina N. V., Ushakov V. A., Rudina N. A., Rogov V. A., Kuznetsov V. V., Lazarchuk V. V., Balakhonov V. G., Matyukha V. A., Drobyaz A. I., Khlytin A. L., Preparation and studies of bulk uranium oxide catalysts, III International Conference "Catalysis: Fundamentals and Application" (Proceedings), Vol. 2, Novosibirsk, Russia, July 4–8, 2007, P. 270–271.

131 Agastini G., Ledoux M. J., Hilaire L., Maire G., in: Preparation of Catalysts, IV, Vol. 31, B. Delmon *et al.* (Eds.), Elsevier, Amsterdam, 1987.
132 Ledoux M. J., Hantzer S., Pham Huu C., Guille J., Desaneaux M.-P., New synthesis and uses of high-specific-surface SiC as a catalytic support that is chemically inert and has high thermal resistance, *J. Catal.*, 1988, Vol. 114, No. 1, P. 176–185.
133 Ismagilov Z. R., Kuntsevich S. V., Shikina N. V., Kuznetsov V. V., Kerzhentsev M. A., Ushakov V. A., Rogov V. A., Boronin A. I., Zaikovsky V. I., Characterization of alumina-supported uranium oxide catalysts in methane oxidation, *Catal. Today*, 2010, Vol. 157, No. 1–4, P. 217–222.
134 Shikina N. V., Ismagilov Z. R., Kuntsevich S. V., Rogov V. A., Ushakov V. A., Boronin A. I., Zaikovskii V. I., Rudina N. A., Kuznetsov V. V., Lazarchuk V. V., Balakhonov V. G., Matyuha V. A., Drobyaz A. I., Khlytin A. L., Study of an influence of preparation conditions of alumina supported uranium oxide catalysts on their catalytic and physicochemical properties, III International Conference "Catalysis: Fundamentals and Application" (Proceedings), Vol. 2, Novosibirsk, Russia, July 4–8, 2007, P. 89–90.
135 Lazareva S. V., Synthesis and research of uranium oxide catalysts, Abstract of the Candidate's Dissertation in Chemical sciences, Tomsk, 2011. (in Russ.).
136 Hutchings G. J., Taylor S. H., Hudson I. D., A new class of uranium oxide based catalysts for the oxidative destruction of benzene and butane volatile organic compounds, Symposium on Heterogeneous Hydrocarbon Oxidation, Preprint, *ACS Div. Petr. Chem.*, 1996, Vol. 41, P. 106–109.
137 Hutchings G. J., Heneghan C. S., Hudson I. D., Taylor S. H., A new class of uranium oxide based catalysts for the oxidative destruction of benzene and butane volatile organic compounds, in: Heterogeneous Hydrocarbon Oxidation, B. K. Warren and S. T. Oyama (Eds.), *ACS Symp. Ser.*, 1996, Vol. 638, P. 58–75.
138 Hutchings G. J., Heneghan C. S., Hudson I. D., Taylor S. H., Uranium-oxide-based catalysts for the destruction of chloro-organic compounds, *Nature*, 1996, Vol. 384, P. 341–343.
139 Hutchings G. J., Heneghan C. S., Taylor S. H., Hudson I. D., The catalytic combustion of volatile chloro-organic compounds using uranium oxide catalysts, Symposium on Catalytic Combustion, Preprint, *ACS Div. Petr. Chem.*, 1997, Vol. 42, No. 1, P. 142–145.
140 Hudson I. D., Heneghan C. S., Hutchings G. J., Taylor S. H., 90th Ann. Meeting Air Waste Management Assoc. (Proceedings), Toronto, Canada, June, 1997. P. 1–12.
141 Hutchings G. J., Taylor S. H., Hudson I. D., Designing heterogeneous oxidation catalysts, *Stud. Surf. Sci. Catal.*, 1999, Vol. 121, P. 85–92.
142 Hutchings G. J., Taylor S. H., Designing oxidation catalysts, *Catal. Today*, 1999, Vol. 49, No. 1–3, P. 105–113.
143 Heneghan C. S., Hutchings G. J., O'Leary S. R., Taylor S. H., Boyd V. J., Hudson I. D., A Temporal analysis of products study of the mechanism of VOC catalytic oxidation using uranium oxide catalysts, *Catal. Today*, 1999, Vol. 54, No. 1, P. 3–12.
144 Taylor S. H., Heneghan C. S., Hutchings G. J., Hudson I. D., The activity and mechanism of uranium oxide catalysts for the oxidative destruction of volatile organic compounds, *Catal. Today*, 2000, Vol. 59, No. 3–4, P. 249–259.
145 Taylor S. H., O'Leary S. R., A study of uranium oxide based catalysts for the oxidative destruction of short chain alkanes, *Appl. Catal. B. Environmental*, 2000, Vol. 25, No. 2–3, P. 137–149.
146 Taylor S. H., Harris R. H., Hutchings G. J., Hudson I. The activity, mechanism and water as a promoter of uranium oxide catalysts for destruction of volatile organic compounds, in: Interfacial Applications of Environmental Engineering, *Surfactant Science Series*, Vol. 108, M. A. Keane (Ed.), Marcel Dekker, New York, 2002, P. 215–230.
147 Harris R. H., Boyd V. J., Hutchings G. J., Taylor S. H., Water as a promoter of the complete oxidation of volatile organic compounds over uranium oxide catalysts, *Catal. Lett.*, 2002, Vol. 78, No. 1–4, P. 369–372.
148 Taylor S. H., Hutchings G. J., Palacio M.-L., Lee D. F., The partial oxidation of propane to formaldehyde using uranium mixed oxide catalysts, *Catal. Today*, 2003, Vol. 81, No. 2, P. 171–178.
149 Ismagilov Z. R., Kuntsevich S. V., Kuznetsov V. V., Shikina N. V., Kerzhentsev M. A., Rogov V. A., Ushakov V. A., Characterization of new catalysts based on uranium oxides, *Kinetics and Catalysis*, 2007, Vol. 48, No. 4, P. 511–520.
150 Pat. RF No. 2350386, 2007.
151 Green M. L. H., Lago R. M., Total oxidation of chlorinated hydrocarbons by copper and chlorine based catalysts, *J. Chem. Soc., Chem. Commun.*, 1995, No. 3, P. 365–366.
152 Kuznetsov V. V., Ismagilov Z. R., Shikina N. V., Kuntsevich S. V., Ostrovsky Yu. V., Zabortsev G. M., Lazarchuk V. V., Balakhonov V. G., Matyuha V. A., Drobyaz A. I., Khlytin A. L., Uranium oxide catalysts for deep oxidation of chlorinated organic compounds, III International Conference "Catalysis: Fundamentals and Application" (Proceedings), Vol. 2, Novosibirsk, Russia, July 4–8, 2007, P. 274–275.
153 Lazareva S., Ismagilov Z., Kuznetsov V., Shikina N., Kerzhentsev M., Uranium oxide catalysts: Environmental applications for treatment of chlorinated organic waste from nuclear industry, *Environ. Technol.*, 2019, Vol. 40, No. 14, P. 1881–1889.
154 Shikina N. V., Ismagilov Z. R., Kuntsevich S. V., Rogov V. A., Ushakov V. A., Boronin A. I., Zaikovskii V. I., Kuznetsov V. V., Preparation and catalytic activity of nanosized uranium oxides supported on alumina, EuropaCat-VIII "From Theory to Industrial Practice" (Proceedings), Turku/Abo, Finland, Aug. 26–31, 2007.
155 Kuntsevich S. V., Shikina N. V., Kuznetsov V. V., Ismagilov Z. R., Ostrovsky Yu. V., Zabortsev G. M., New uranium oxide catalysts for cleaning of plant emissions from volatile organic compounds including chlorine-containing ones, All-Russian Conference with International Participation "Catalytic Technologies of Environmental Protection for Industry and Transport" (Proceedings), Saint-Petersburg, Russia, Dec. 11–14, 2007, P. 123. (in Russ.).
156 Maximum permissible concentrations (MPC) of harmful substances in the air of the working area, GN 2.2.5.687-98, Hygienic standards, Izd-vo Ministry of Health of Russia, Moscow, 1998. (in Russ.).
157 Radiation safety standards (NRB-99/2009), 2.6.1.2523-09, Izd-vo Ministry of Health of Russia, Moscow, 2009. (in Russ.).
158 Basic sanitary rules for ensuring radiation safety, (OSPORB-99/2010), SP 2.6.1.2612-10, Izd-vo Ministry of Health of Russia, Moscow, 2010. (in Russ.).
159 Basic rules for accounting and control of nuclear materials, Order of Rostechnadzor, NP-030-12, April 17, 2012, No. 255. (in Russ.).